Journal of Building Engineering 121 (2026) 115623

Contents lists available at ScienceDirect

Journal of Building Engineering

journal homepage: www.elsevier.com/locate/jobe

A comprehensive life cycle assessment of vacuum insulation panels (VIPs) for applications at up to 70 °C

Tarek Raad [a], Harjit Singh [a,*], Suresh Sivan [b]

[a] Department of Mechanical and Aerospace Engineering, College of Engineering, Design and Physical Sciences, Brunel University London, Uxbridge, UB8 3PH, United Kingdom

[b] Department of Mechanical Engineering, National Institute of Technology, Tiruchirappalli, Tamil Nadu, 620015, India

ARTICLE INFO

Keywords:
Life cycle assessment
Impact categories
Vacuum insulation panel (VIP)
Natural fibres
Tree waste
Car painting booth
Thermal conductivity

ABSTRACT

This paper presents a comprehensive Life Cycle Assessment (LCA) of Vacuum Insulation Panels (VIPs) with four core materials: fumed silica (FS) and three FS-based composites incorporating tree-based natural fibre (TNF) waste and tree-based natural ash (TNA), using a typical car painting booth (CPB) as a case study. A cradle-to-cradle evaluation is performed using two functional units: material transport capacity (6.2 tonnes per truck) and VIP dimensions (1 m × 1 m × 25 mm). VIPs were manufactured and their thermal conductivity measured over pressures of 0.64–1000 mbar and temperatures of 20–70 °C. Ageing effects were assessed by storing VIPs at 70 °C and 75% relative humidity for 12 months. Measured thermal conductivities were used to predict CPB energy consumption over a 10-year operational lifetime. Results show that FS–TNA VIPs (S4) reduced total cradle-to-cradle energy demand by 82,761 MJ compared with FS VIPs (S1) using Cut-off approach. However, this energy benefit did not translate into a climate advantage, as S4 exhibited a higher climate change impact of 893 kg CO_2 eq, primarily due to pyrolysis-related emissions. Under the Allocation at Point of Substitution (APOS) approach, S4 reduced total energy demand by 17,216 MJ and climate change impact by 141 kg CO_2 eq relative to FS, reflecting both operational energy savings and avoided biomass degradation emissions. When expressed per unit of energy saved relative to S1, S4 resulted in 55.0 kg CO_2 eq per GJ under the modified Cut-off scenario used as the main modelling approach in this study, and (−) 8.2 kg CO_2 eq per GJ under the modified APOS scenario used as an alternative allocation approach, highlighting the scenario-dependent energy–climate trade-off. Overall, the study demonstrates that trade-offs between embodied emissions, operational energy demand, and end-of-life modelling influence VIP environmental performance and provides a transparent methodology to support material selection for high-temperature industrial applications.

1. Introduction

The UK Government has aims to completely decarbonise electricity generation by 2035 and to decrease energy usage in buildings by a minimum of 15% by 2030 by adopting improved energy efficiency measures [1]. Insulation is seen as a crucial element in reaching these goals by enhancing energy efficiency in buildings through the reduction of energy demand for heating and cooling, hence decreasing greenhouse gas emissions. Several insulation materials are presently utilised in the UK, including Expanded Polystyrene

* Corresponding author.
E-mail address: harjit.singh@brunel.ac.uk (H. Singh).

https://doi.org/10.1016/j.jobe.2026.115623
Received 19 November 2025; Received in revised form 8 February 2026; Accepted 13 February 2026
Available online 18 February 2026

(EPS), fibreglass, and mineral wool, exhibiting thermal conductivities ranging from 30 to 40 mW m^{-1} K^{-1} [2–4]. It is increasingly becoming more and more evident that these materials would struggle in meeting the newly set environment targets, particularly concerning their thermal conductivity during usage phase and impacts on the environment during production and disposal phases.

For example, policy drivers such as Energy Performance of Buildings Directive (EPBD), require the European Union to achieve a 32.5% increase in energy efficiency by 2030 in all sectors [5]. Moreover, the UK prohibited the use of EPS in food-related applications as of November 2023 [6]. This legislative change indicates a possibility of similar restriction(s) in industry sector as well. This legislative change suggests a trajectory toward more stringent regulation of EPS across broader applications, including its industrial use. In this context, industrial thermal enclosures, such as Car Painting Booths (CPBs), are increasingly being scrutinised through the same lens as building. Although CPBs are technically process equipment, they are enclosed, thermally regulated spaces located within or attached to buildings. In 2023, the UK automotive sector consumed 3.128 TWh of electricity and emitted a total of 603,319 tonnes of CO_2 during the vehicle production phase [7]. Out of the total energy consumed, 20–30% is attributed to the oven process, primarily CPBs, which necessitate maintaining precise temperatures (up to 70 °C) within the booth [8].

Vacuum Insulation Panels (VIPs) have generated a huge interest in recent years due to their ability to achieve a thermal conductivity of less than 0.007 W m^{-1}. K^{-1} [9], which is 3-7 times smaller than that of conventional insulation. Understandably, they possess a notable advantage in terms of space economy, since VIPs require a relatively thinner sections compared to conventional insulation to deliver a given U-value [10]. In cold chain logistics, VIPs minimise heat loss and substantially decrease the energy required for refrigeration [11]. Additionally, other researchers are investigating the usage of VIPs in higher temperature applications, exploring their potential to enhance thermal insulation in various industries [12,13].

The advantages of VIPs when used in construction [14] and several other sectors have been examined and presented. However, their lifecycle scale environmental impact has not been paid sufficient attention with only a few studies reported to date showing that the fumed silica (FS) core dominates the environmental footprint of VIPs, accounting for up to ~90% of total impacts due to energy-intensive production and material processing [15–17]. High cost of core materials (up to 60% of the total) is another major challenge [18]. Furthermore, it is crucial to investigate the reusability of VIP core materials. Initiatives that improve reusability and diminish waste can substantially elevate the overall sustainability of these panels [19,20].

Consequently, there is an increasing emphasis on developing alternative core materials, such as Natural Fibres (NFs), bamboo, straw, wood pulp and wood fibre, that are thermo-physically useable in VIPs [21–25]. However, these materials are needed to be critically investigated for their environmental and cost creditworthiness. The current study fulfils this knowledge gap by systematically evaluating several alternative core materials, encompassing both organic and inorganic candidates, to produce sustainable VIPs. Life-cycle assessments (LCA) of VIPs has been conducted. The study involves examination of research that defines functional units, identification of system boundaries and assessment of critical parameters affecting environmental impacts.

This paper presents a novel, application-driven approach to assessing the environmental impacts of Fumed Silica (FS) and its composites with tree-based waste-derived natural fibres and ash. In total, four core materials were investigated using a high-temperature industrial case study, namely a Car Painting Booth (CPB). Two distinct LCAs were conducted employing two complementary functional units: one based on the raw material quantity transported (truck load capacity of 6.2 tonnes), referred to as the "Core LCA", and another based on VIP dimensions (1 m × 1 m × 25 mm), referred to as the "VIP LCA". The study provides a comprehensive analysis of how resources used in VIP production, assessed using the Cumulative Energy Demand (CED) method, influence climate change impacts as defined by the EN 15804 + A2 standard. Life-cycle impacts, including climate change, acidification, land use, and both renewable and fossil energy consumption, are examined for the different core materials. Other EN 15804 + A2 impact categories were not included because a preliminary screening indicated that they were not dominant for this system and did not influence the comparative ranking of the studied scenarios. Experimental measurements of thermal conductivity were conducted at varying pressures and temperatures, alongside an ageing study and an evaluation of core material reuse potential. To quantify operational energy savings, a CPB energy model was developed using COMSOL Multiphysics. In addition, the study explores the long-term environmental performance of VIPs under future UK energy scenarios extending beyond the 2050 net-zero target, using both Cut-off and Allocation at Point of Substitution (APOS) approaches to capture the effects of waste utilisation and reuse. By directly linking experimentally measured ageing behaviour with operational energy modelling and dual-functional-unit LCA, this work addresses key gaps in existing studies that typically focus on building-scale applications and decouple thermal performance from life-cycle assessment. This investigation therefore enhances transparency in LCA practice by clarifying how modelling choices, databases, and allocation approaches influence the environmental evaluation of VIPs.

2. Hybrid methodology

The methodological framework of ISO 14040:2006 [26] was followed for goal and scope definition, life cycle inventory analysis, life cycle impact assessment and result interpretation. The LCA is structured in two assessments. The first phase (Core LCA) examines the cradle-to-gate environmental impacts of extracting and processing fumed silica (FS) and tree-based natural fibre waste. The functional unit for this phase is determined based on the load capacity of a typical lorry, which is 6.2-tonnes, to cover the transportation of raw materials from the source (mine or woods) to the manufacturing facility. The second phase (VIP LCA) expands the scope to a cradle-to-cradle assessment, covering raw material extraction, production, usage, disposal, and reuse potential of different VIP core materials utilised in CPB. The functional unit for this phase is defined as a VIP with a cross-section area of 1 m^2 (thickness of 25 mm) to imitate a typical commercially available VIP. While the two functional units may appear distinct, they are purposefully chosen to suit different phases of the product life cycle. The LCA was structured in two stages to improve transparency, allowing the contribution of materials to be quantified separately rather than aggregated into a single cradle to cradle inventory. The Core LCA

adopts a transport-oriented unit (6.2 tonnes) to capture cradle-to-gate impacts and reflect real-world logistics scenarios. In contrast, the VIP LCA uses a surface-based unit (1 m^2 panel at 25 mm thickness), which serves as a practical and consistent basis for evaluating insulation performance in application. This area-based unit is later linked to thermal performance via experimentally measured thermal conductivity and energy simulation in a CPB environment. Together, the two units provide complementary insights, one focused on production and transport efficiency, and the other on application-level environmental performance of different VIPs. Results from the core LCA (6.2-tonne functional unit) were scaled according to the mass of core material used per VIP and directly integrated into the VIP LCA inventory (1 m^2 functional unit). The Core LCA results are presented solely to improve upstream traceability and transparency and should not be interpreted independently of their scaling into the application-based VIP functional unit.

As a precursor to this study, FS and tree-based natural fibres with average fibre lengths of 0.82 mm and 0.22 mm, designated as TNF1 and TNF2, respectively, were processed and optimised to produce VIPs with FS in the laboratory. The findings have been published [27]. Additionally, this study introduces a novel core material derived from the controlled partial pyrolysis of residual tree-based materials (after sieving), termed as Tree-based Natural Ash (TNA); the methodology followed for the development of TNA, in addition to the Scanning Electron Microscopy (SEM) and Mercury Intrusion Porismetry (MIP) of all samples are presented in Appendix A. VIPs were manufactured using an in-house vacuum sealing machine, incorporating composites comprising 70 wt% FS and 30 wt% TNF1 or TNF2 or TNA. Thermal conductivity of the manufactured VIPs was measured using a Netzsch heat flow meter [28] at variant mean temperatures (20, 40, 50 and 70 °C) and pressures, see Table 1.Internal pressure was measured using the foil lift-off method and is reported as the mean ± standard deviation of three repeated measurements. The loose powder of these different materials is presented in Fig. 1. Additionally, the ageing effects of all samples were evaluated under controlled conditions (70 °C & 75% relative humidity). To assess reusability, FS and composite samples were unsealed after six months of storage under controlled room conditions (20 °C & 40% relative humidity) and repurposed as new core materials to examine the impact of compaction and long-term storage. Among the investigated samples, S1 (FS) and the three optimised VIP core compositions, S2 (FS-TNF1), S3 (FS-TNF2) and S4 (FS-TNA), were investigated as potential alternatives to the commonly used Expanded Polystyrene (EPS) insulation in CPB, which requires a drying chamber temperature of 70 °C. Total energy savings from the use of VIPs against EPS insulation were calculated assuming a CPB life of 10 years whilst considering the rise in VIP thermal conductivity due to ageing effect. Full model specification of CPB including boundary conditions, turbulence and radiation models, mesh configuration, and convergence testing, is provided in Appendix B. Fig. 2 presents a conceptual system boundary diagram illustrating the life-cycle stages and processes considered in this study, rather than a detailed quantitative flow representation; the corresponding quantitative results and life-cycle impact outcomes are presented and discussed in Section 3.

2.1. LCA system boundary and approaches

The general life cycle stages of conventional insulation material are described in the European standards (Pargana et al., 2014). According to these regulations, the system boundaries are typically categorised into three main groups – cradle-to-gate (A1-A3), cradle-to-grave (A1-C4) and cradle-to-cradle (A1-D). However, these general stages fail to capture specific steps involved in the VIP lifecycle due to it being a comparatively new insulation material and often lack of knowledge and information about it among researchers. To address this knowledge gap in order to achieve more precise and realistic outcomes genuine environmental consequences of processing the core material, which serves as the primary component of VIPs, were assessed. Transparency and traceability are ensured by segmenting life stages into various components with the boundaries delineated in Table 2.

Attributional LCA (ALCA) using the Cut-off approach was conducted and going a step forward compared with Allocation at Point of Substitution (APOS) approach [31]. The Cut-off model assesses the immediate impacts of manufacturing, usage, and disposal, excluding the advantages of recyclability [32]. The APOS methodology distributes environmental impacts uniformly, acknowledging collective responsibility [33].

2.2. LCA inventory analysis

The database of SimaPro Software (version 10.2) was used to evaluate the energy consumed in the development of the core material and the manufacture of VIPs using the Cumulative Energy Demand (CED) and the EN15804 + A2 methods, as the work was conducted in the United Kingdom.

Current data was employed in this study to realistically reflect the electricity mix in the UK wherein generation, transmission losses and emissions were accounted for. Fossil fuels supplied 46% of total energy use, with natural gas as the primary contributor, and renewables 19%. Data from the International Energy Agency (IEA) and Ecoinvent provided insights into electricity mix shifts between

Table 1
Different VIPs made from core composition of tree based natural fibre and fumed silica and their relevant measured pressure.

Sample ID	Fumed Silica (FS)	Tree based waste			Pressure (mbar)
		TNF1	TNF2	TNA	
S1	100				1.5 ± 0.15; 10 ± 1.2; 97 ± 7.8; 1000
S2	70	30			0.6 ± 0.08; 15 ± 1.4; 132 ± 16; 1000
S3	70		30		1.6 ± 0.21; 14 ± 1.7; 155 ± 19; 1000
S4	70			30	2.8 ± 0.25; 10 ± 1.3; 94 ± 10; 1000

Fig. 1. Photographs of the materials used in this study - (a) S1, (b) S2, (c) S3 and (d) S4.

2016 and 2022, revealing a decline in coal and nuclear and a rise in wind and solar energy; data is presented in Appendix C. This method clearly addresses the drawbacks of the CED method, established in the early 1970 and rarely updated [34].

Initially, using the EN 15804+A2 methodology, climate change, acidification, and land use impacts were calculated using the existing database in SimaPro [35]. Carbon dioxide from the burning of fossil fuels was found to be the major contributor to climate change (86%), while acidification was primarily driven by sulphur dioxide and nitrogen oxides (93%). Subsequently, the study recalculated emissions based on updated IEA 2022 data by adjusting CED values and revising impact estimates for 1 MJ of electricity. The results, seen in Table 3, showed that reduced fossil fuel dependency decreased climate change and acidification impacts in both Cut Off and APOS approaches. The environmental effects of renewable energy production were not considered in this analysis.

Fumed silica used in this study was procured from commercial suppliers, but the complete processing of tree-based natural fibres and the manufacturing of the VIP were conducted in Brunel labs. It is crucial to note that the manufacturing processes adopted are similar to those used by commercial VIP manufacturers. Understandably, the quantity of materials used significantly differs between both cases. Despite a lot of interest, there is no commercial TNF based VIP product in the market to date. This necessitated utilisation of secondary data by raising laboratory data to industrial processes and equipment. Fumed silica was studied using the procedure and basic data provided in Resalati et al. (2021) [36]. Input data concerning energy required for packaging, diesel processing and envelope and fleece were sourced from SimaPro library using the revised energy mix data from CED. The inventories and the input data used in the core and the VIP LCA studies are presented in Tables 4 and 5 respectively. Tree-based natural fibres (TNF) were modelled as a waste-derived material. In line with the cut-off approach (ISO 14044; EN15804), no upstream burdens from tree growth or harvesting were assigned at the point of waste generation. All subsequent processes (i.e., collection, drying, grinding, sieving, packaging, and transport) were fully included in the life-cycle inventory (Table 4). Accordingly, TNF is not treated as impact-free beyond the waste boundary; only the original biomass production is excluded. To account for variability, two transport distances were modelled: 200 miles was assumed for raw material transportation between suppliers and manufacturing facilities, while 500 miles was assumed for the transportation of finished VIPs from manufacturing sites to CPB locations. Diesel consumption values were based on real-world freight data, and a custom transport model was developed using Mercedes-Benz Actros L specifications and IPCC (2023) emission factors, as detailed in Appendix C. These assumptions are considered reasonable for UK-based supply chains and serve to illustrate the environmental impact across variant logistics scenarios.

The energy requirement to produce TNA by pyrolysis was calculated from the experimental processing conditions and furnace energy consumption. Direct measurement of gaseous emissions during pyrolysis was not conducted. Instead, emissions of CO_2 and CH_4 were estimated using a chemistry-based stoichiometric approach grounded in the known composition of tree-based biomass. Tree-based fibres consist primarily of cellulose, hemicellulose, and lignin. Emissions were calculated based on the decomposition reactions of cellulose and hemicellulose according to established formulations, yielding quantified amounts of CO_2 and CH_4 per kilogram

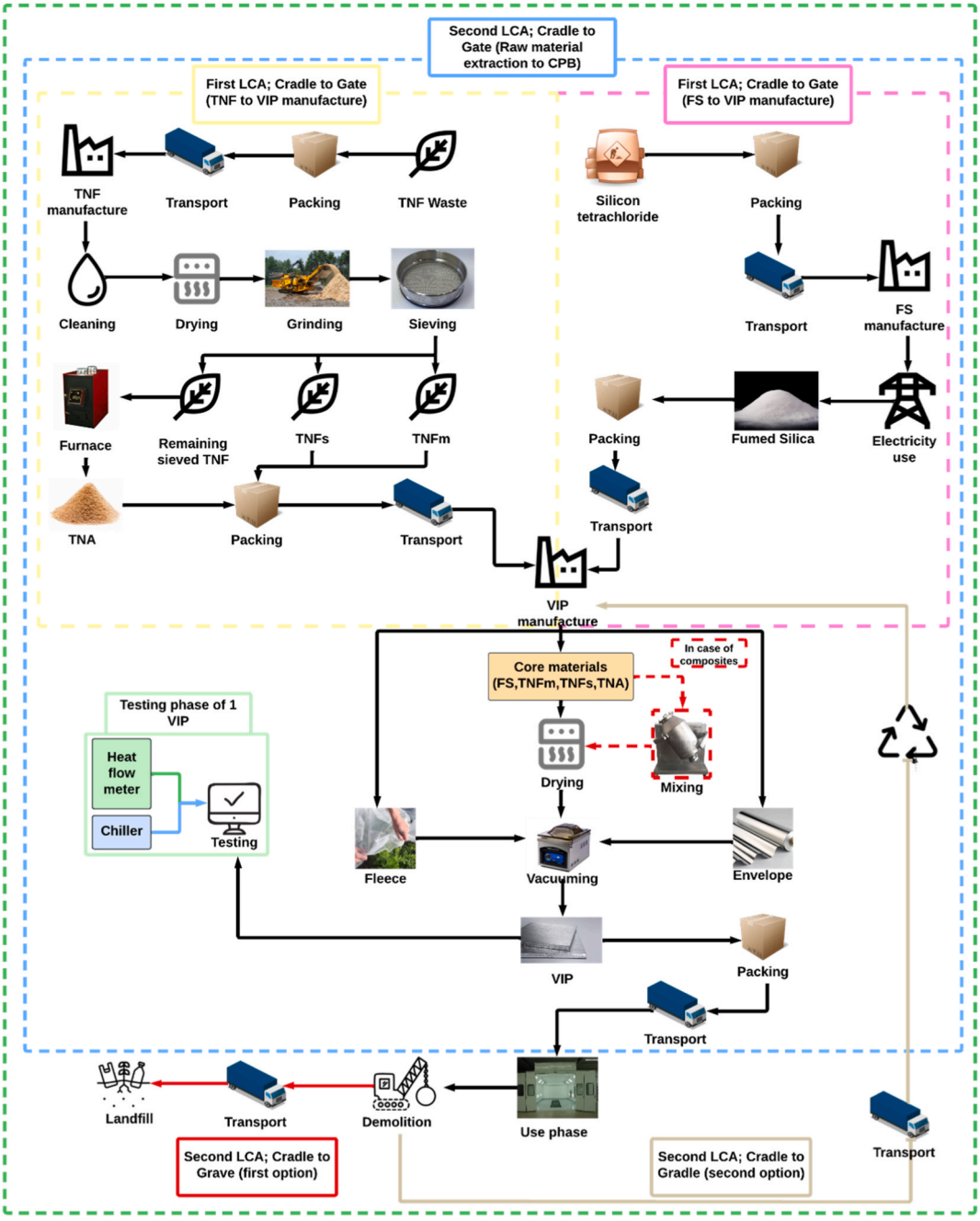

Fig. 2. System boundary and life-cycle phases of VIPs.

of material processed. Lignin was assumed to be largely resistant to degradation over the time horizon considered. This approach enabled the incorporation of process-specific emissions into the life-cycle inventory without relying on generic database proxies. Full derivations and assumptions are provided in Appendix C.

The envelope and fleece inventories (mass and energy demand) were sourced directly from the SimaPro database, using representative multilayer polymer–aluminium composite and textile processes, due to the absence of supplier-disclosed material specifications.

2.3. Limitations and uncertainties of the study

The following limitations and uncertainties were identified.

Table 2
LCA boundaries and life cycle stages of VIP based on the EN 15978 and EN 15804 European standards [29].

Life cycle stage and description	System boundaries
A1.1 - Raw material extraction	Quantity of tree waste material - 6105.2 kg Amount of silicon tetrachloride ($SiCl_4$) – 5920 kg
A1.2 - Packing of raw material	Folding carton cardboard: • Dimension: 0.6 x 0.4 × 0.4 m^3 • Weight: 0.5 kg Tree-based natural fibres density: 1200 kg m^{-3} Intermediate Bulk Containers (IBCs): • Capacity: 1000 L (Kurasov, 2009) • Weight: 60 kg $SiCl_4$ density: 1480 kg m^{-3} [30]
A2 - Transport to the core manufacturing facility (transportation 1)	Distance travelled: 200 miles Truck load: 6.2-tonnes (first FU) Truck Capacity: 33 m^3
A3.1 - Raw material processing	Processing of TNF into TNF1, TNF2 and TNA Processing $SiCL_4$ into FS
A3.2 - Packing and transport to VIP manufacturing facility (transportation 2)	TNF1 (ρ: 310.4 kg m^{-3}) and TNF2 (ρ: 212.6 kg m^{-3}) packed in 58 and 33 folding carton cardboards, respectively TNA (ρ: 356.1 kg m^{-3}) and FS (ρ: 52.6 kg m^{-3}) packed in 23 and 1031 fertiliser bags, respectively Distance travelled: 200 miles
A1.1 to A3.2 covered the full process from raw material extraction to VIP manufacturing gate (cradle-to-gate of the Core LCA).	
A3.3 - Manufacturing of VIPs	The environmental impact of manufacturing a 1 m^2 VIP (second FU), including testing of VIPs.
A4 - Packing and transport the manufactured VIPs to the CPB (transportation 3)	128 manufactured VIPs Folding carton cardboard: • Dimension: 1.1 x 1.1 × 0.2 m^3 • Weight: 0.5 kg • Count: 32 Distance travelled: 500 miles
A1.1 to A4 concludes the first part of the VIP LCA study, covering the environmental impact from raw material extraction to the CPB site (cradle-to-gate).	
B1 - Installation of VIPs in the CPB	Use of 200 g of polyurethane adhesive Human activity was not considered
B6 - Operational energy use of the CPB	Examination of energy used in CPB insulated with VIPs against EPS over a decade Although maintenance (B2), repair (B3), replacement (B4), refurbishing (B5), and water consumption (B7) were excluded because VIPs are assumed to be maintenance-free and water-free, ageing effects were explicitly accounted for through time-dependent thermal conductivity (Section 3.2), which captures performance degradation over the service life without assuming physical intervention
C2.1 - Transport to disposal site (transportation 4)	Demolition (C1) was excluded Transport of VIPs to a designated disposal site (500 miles)
C2.2 - Transport back to VIP manufacture (transportation 4)	Demolition (C1) was excluded The transport of only the used core materials back to the VIP manufacturing facility (500 miles)
C4 – Disposal	Disposal of all VIP components Specific focus on the environmental effects of landfilling various core materials
The second part of the VIP LCA study was concluded after this phase, covering all aspects except C2.2 (cradle-to-grave)	
D - Potential reuse of the core material	Beneficial consequences of reusing VIP core materials Environmental advantages and impacts of further usage in the new life cycle
The full life cycle of VIPs was concluded after this phase, excluding C2.1 and C4 (cradle-to-cradle)	

C2.1 (transport to disposal) and C2.2 (transport back to manufacture) represent alternative end-of-life pathways and are applied exclusively to cradle-to-grave and cradle-to-cradle scenarios, respectively. C4 (disposal) is included only in cradle-to-grave modelling; in cradle-to-cradle scenarios, all VIP components are assumed to be reused and therefore do not undergo final disposal.

Table 3
The amended values and the SimaPro values for acidification and climate change impacts in different system approaches.

Impact category	Cut-off		APOS	
	SimPro Value	New Value	SimPro Value	New Value
Acidification	2.87E-04	2.76E-04	3.11E-04	2.87E-04
Climate change	8.42E-02	4.88E-02	9.97E-02	6.64E-02

- Inventory data quality: Primary data were sourced from lab experiments and secondary literature. TNF processing is not commercialised, so equipment power and outputs were scaled to industrial levels, introducing uncertainty due to the lab-to-industry extrapolation.
- Assumptions and simplifications: Equal transport distances were assumed for all stages to ensure consistency. Only TNF contributed to landfill emissions due to cellulose degradation, while FS was assumed inert. Envelope and fleece data were sourced from SimaPro, which may carry inaccuracies.

Table 4
The life cycle inventory used in the core LCA.

The core LCA	FS		TNF1		TNF2		TNA	
	Amount (kg)	Energy (MJ/kg)	Amount (kg)	Energy (MJ/kg)	Amount (kg)	Energy (MJ/kg)	Amount (kg)	Energy (MJ/kg)
Folding carton cardboard	-	-	26.5	13.9	26.5	13.9	26.5	13.9
Silicon tetrachloride	5920	8.5	-	-	-	-	-	-
Production of FS	2190	16.5	-	-	-	-	-	-
Intermediate Bulk Containers	240	19.6	-	-	-	-	-	-
Diesel for transportation 1	144.6	33.1	144.6	33.1	144.6	33.1	144.6	33.1
Drying	-	-	6105.2	0.09	6105.2	0.09	6105.2	0.09
Grinding	-	-	6105.2	0.03	6105.2	0.03	6105.2	0.03
Sieving	-	-	6105.2	0.0003	6105.2	0.0003	6105.2	0.0003
Pyrolysis	-	-	-	-	-	-	3724.2	0.78
Packing of processed material	515.5	1.1	29	13.9	16.5	13.9	11.5	1.1
Diesel for transportation 2	144.6	33.1	144.6	33.1	144.6	33.1	144.6	33.1

*Energy values are reported as specific energy intensities (MJ per kg of input), consistent with life-cycle inventory conventions.

Table 5
The life cycle inventory of the VIP LCA.

The VIP LCA	Energy needed for one VIP (MJ)			
	S1	S2	S3	S4
Core material (data from the core LCA)	313.7	230.6	310.7	313.7
Mixing	-	0.13	0.14	0.12
Drying	9.3	6.7	6.8	6.6
Vacuuming	1.4	1.4	1.4	1.4
Testing	3.3	3.3	3.3	3.3
Envelope	33.1 MJ for 54 g			
Fleece	1.6 MJ for 30 g			
Packing of VIP	2.9 MJ			
Diesel for transportation 3	20092.6 MJ for 361.5 kg of diesel (128 VIPs)			
Polyurethane adhesive	11.4 MJ for 200 g			
Diesel for transportation 4	20092.6 MJ for 361.5 kg of diesel (128 VIPs)			

- Ecoinvent database constraints: Background LCI data relied on Ecoinvent (cut-off and APOS). Some datasets, such as electricity generation, were outdated (e.g., 2016), and modified using recent IEA data (2022), adding potential uncertainty.
- Life cycle impact assessment methodology reliability: Environmental impacts were assessed using CED and EN15804+A2. Only key categories were retained; minor or irrelevant impacts were excluded. Methodological differences in impact assessment may influence overall results.
- Absence of direct industrial CPB energy data for model validation, due to the unavailability of proprietary manufacturer datasets; therefore, absolute energy values should be interpreted as indicative, while comparative trends remain robust.
- Potential material losses and additional energy associated with dust handling and emission control during fumed silica production were not explicitly modelled due to the lack of publicly available process-specific data and are therefore acknowledged as a source of uncertainty in the upstream inventory.
- Only TNF was assumed to cause environmental impacts at landfill due to cellulosic degradation and associated emissions, while fumed silica was assumed to contribute solely through land occupation based on its density and quantity, as no documented landfill degradation impacts are reported in the literature.
- Disposal and recycling of secondary materials (envelope and fleece) were modelled using SimaPro database processes, which may introduce additional uncertainty due to the use of generic datasets.
- The deterministic approach adopted in this study is considered appropriate because the dominant sources of uncertainty arise from system definition, allocation choices, and end-of-life modelling assumptions rather than background data variability. Under such conditions, stochastic Monte Carlo analysis may introduce a false sense of numerical precision without resolving the underlying scenario-based uncertainties. Therefore, sensitivity analysis was used to reflect the comparative and scenario-oriented objectives of the study.
- It should also be noted that the environmental advantages associated with TNF-based VIPs depend on the continued availability of tree waste as a low-burden input. In cases where tree waste is already utilised in competing applications such as bioenergy, mulching, or soil amendment, the assumed benefits may be reduced or displaced.

3. Results and discussions

Section 3 presents the experimental results, energy modelling, and life cycle assessment outcomes of the studied vacuum insulation panels. It begins with the experimental characterisation of thermal conductivity as a function of temperature (20–70 °C) and internal pressure (0.6–1000 mbar), followed by an ageing assessment of the VIPs stored under controlled conditions (70 °C and 75% relative humidity). The section then examines the performance of reused core materials and evaluates the resulting impact on VIP thermal behaviour. These experimental findings are subsequently integrated into a car painting booth (CPB) energy model to quantify operational energy consumption over a 10-year period while accounting for ageing effects. The section further presents life cycle assessment results across multiple impact categories for cradle-to-gate, cradle-to-grave, and cradle-to-cradle system boundaries, including the influence of CPB operation and thermal performance. The environmental benefits of core material reuse are then analysed, followed by a sensitivity analysis comparing Cut-off and APOS approaches under different energy-mix assumptions. Finally, future LCA projections are presented assuming a net-zero energy system consistent with full energy decarbonisation scenarios.

Uncertainty in thermal conductivity measurements presented in Figs. 3–6 arises primarily from the measurement accuracy and repeatability of the NETZSCH HFM 446 Lambda apparatus, as detailed in Appendix A. All reported values represent the average of repeated measurements conducted under identical conditions, with observed variation remaining within the instrument uncertainty range. As the figures aim to illustrate comparative trends between materials, temperatures, pressures, ageing time, and reuse conditions, additional statistical error propagation was not applied. Control parameters and their ranges were selected to reflect realistic operating conditions for high-temperature industrial applications, particularly car painting booths. Temperatures, pressures, ageing conditions, time horizons, and transport scenarios were defined based on CPB requirements, material performance limits, and literature, and were held constant across all scenarios to ensure consistent comparison.

3.1. VIP thermal conductivity measurements

Experimental measurements were conducted to determine the thermal conductivity of S1 (FS), S2 (FS-TNF1), S3 (FS-TNF2), and S4 (FS-TNA) VIPs at conditions specified in Section 2. Whilst the thermal conductivity values of samples S1, S2, and S3 were detailed and their underlying performance rationale explained [27], results for sample S4 are being presented in this study for the first time. The findings indicated that the S4 exhibited the lowest thermal conductivity of 6.23 mW m^{-1} K^{-1} at 20 °C and 7.41 mW m^{-1} K^{-1} at 70 °C among all samples as shown in Fig. 3. This behaviour is consistent with a similar trend observed in the TNF samples, where the radiative conductivity of S4 was lower than that of S1, contributing to the overall lower thermal conductivity.S4 was also found to have a lower solid conductivity, compared to S2 and S3, which is consistent with the formation of aggregates made of small TNA and FS particles in contrast to the larger, distinctly separated fibre-sized particles of varying lengths found in S2 and S3. The accumulation of particles is consistent with the formation of smaller pores in S4, which may contribute to reduced gas conductivity even under elevated sealing pressures.

At mean temperature of 70 °C, S4 at 94 ± 10 mbar exhibited lower thermal conductivity than S1 at 97 ± 7.8 mbar, as did S2 and S3 at 132.3 ± 16 mbar and 155.1 ± 19 mbar, respectively. The results suggest greater contribution of radiative conductivity to the overall thermal conductivity at high temperatures compared with gaseous conductivity under these internal pressures.

Under atmospheric pressure, S4 demonstrated the lowest thermal conductivity at 23.4 mW m^{-1} K^{-1} succeeded by S1 at 25.0 mW m^{-1} K^{-1}, S3 at 25.5 mW m^{-1} K^{-1} and S2 at 26.2 mW m^{-1} K^{-1}. The results support the fact that gaseous conductivity exerted a more significant influence at atmospheric pressure, exceeding radiative effect, in the case of fibres, see Fig. 4. The thermal conductivity measured in this study fall within the range of performance reported by published manufacturer data at standard conditions (23 °C and

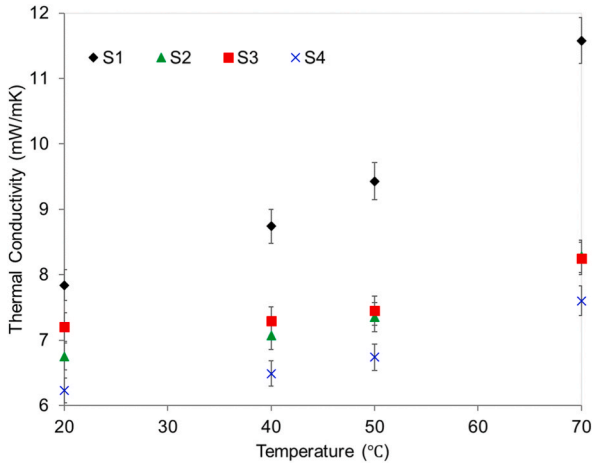

Fig. 3. Thermal conductivity of samples S1–S4 at internal pressures of 1.5 ± 0.15 mbar (S1), 0.6 ± 0.08 mbar (S2), 1.6 ± 0.21 mbar (S3), and 2.8 ± 0.25 mbar (S4).

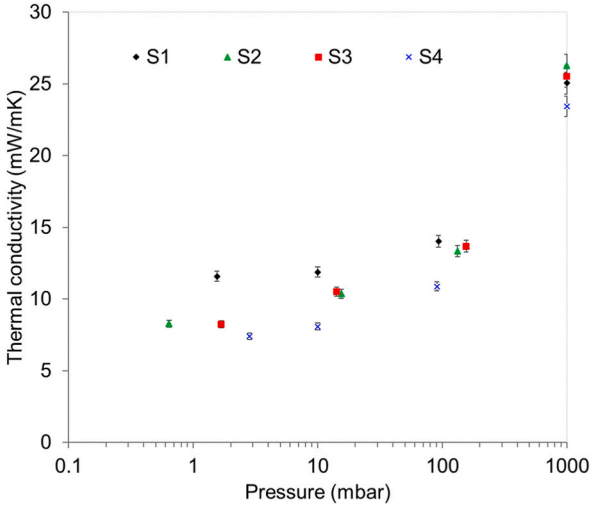

Fig. 4. Thermal conductivity of four manufactured samples at a mean temperature of 70 °C.

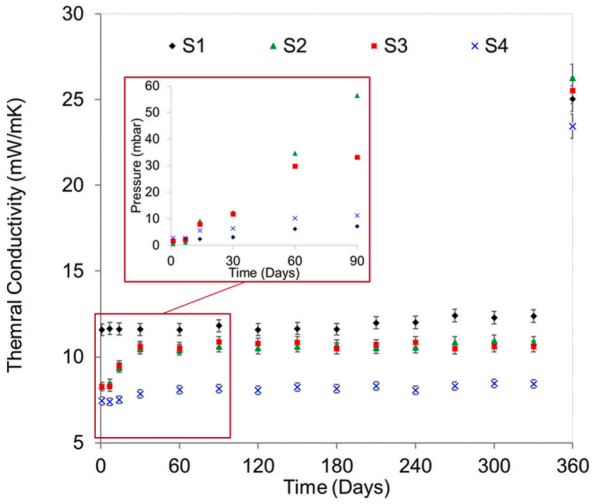

Fig. 5. Ageing thermal conductivity of four manufactured VIPs under storing conditions of 70 °C and 75 % RH and measured variation of pressure over 90 days.

50% RH).

3.2. *Ageing performance*

The thermal conductivity of VIPs increased over time influenced by the core and envelope materials. FS is hydrophobic while TNF-based materials are hydrophilic.

All VIPs were sealed at low pressures (0.6 – 2.8 mbar) and stored under controlled conditions (70 °C, 75 % relative humidity). Thermal conductivity was measured at predetermined discrete time points - immediately after manufacturing, 7 days after manufacture and 30 days after manufacture followed by monthly measurements for 12 months. Equation (1) was used to forecast the rate of increase in conductivity over a decade, identifying the time needed for a 5 mW m^{-1} K^{-1} rise (a significant impact on booth performance) and a 17 mW m^{-1} K^{-1} rise (indicating envelope failure).

$$r = \frac{\lambda(t) - \lambda 0}{t} \tag{1}$$

where r is the rate of increase of thermal conductivity, $\lambda(t)$ the thermal conductivity measured at a given time, $\lambda 0$ the thermal conductivity measured immediately after manufacturing and t the time.

Samples containing TNF materials (S2 and S3) exhibited a significant increase in overall thermal conductivity over time. The reason

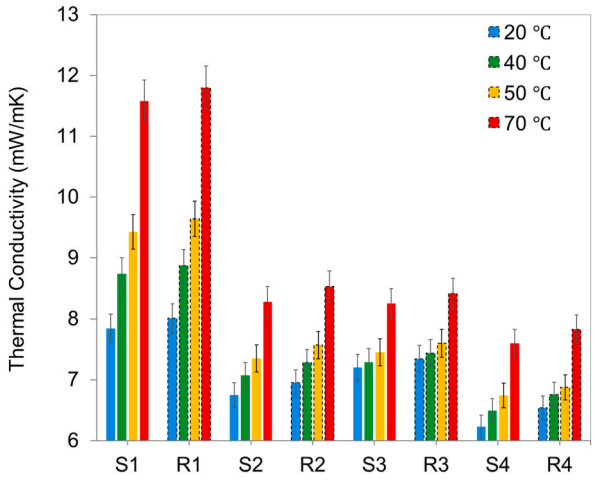

Fig. 6. Comparison of thermal conductivity of original core VIPs with reused core VIPs.

behind it was ascribed to outgassing from TNF which contains cellulose, hemicellulose, and lignin and tend to retain residual moisture. The trapped moisture can gradually evaporate under elevated temperature conditions, resulting in an increased pressure and therefore, a higher thermal conductivity, see Fig. 5.

On the other hand, the pyrolysis to produce TNA at high temperature, resulted in the decomposition of components like cellulose and hemicellulose into substances such as CaO, Na2O, and P_2O_5. These chemical compounds are recognised for their hygroscopic properties, enabling them to attract and retain moisture even under low environmental conditions. The presence of these compounds (approximately 18%) is linked to the gradual increase of thermal conductivity over time. However, the overall conductivity increase rate for TNA samples was lower than that of TNF samples, indicating that VIPs with TNA may deliver a longer useful lifespan under similar storage conditions.

The envelope utilised for VIPs (metallised multi-layered PET) was considered unsuitable for prolonged use in applications like a car painting booth, which operates at an average operating temperature of 70 °C. It was unjust to evaluate the ageing of various core materials based on envelope failure. The study aimed to focus on the impact of core material ageing by calculating the total increase thermal conductivity just before the envelope got damaged (330 days).The results were more realistic with this approach, since different envelopes with greater moisture resistance may be utilised in such applications. It should be noted that the ageing behaviour reported here is specific to the tested envelope material and sealing conditions, and should not be extrapolated to all VIP designs, as different envelope systems may lead to substantially different ageing rates. Table 6 displayed the years for the four measured samples to increase by 5 mW m^{-1}. K^{-1} and 17 mW m^{-1} K^{-1}.

3.3. Reused cores

All S1, S2, S3 and S4 samples, stored at room temperature of 20 °C and relative humidity of 40%, were unsealed after a period of 6 months following production. These VIP samples were reopened, and their cores were reused to produce new VIPs using a 3D mixer. The remade samples were designated as 'R', following the abbreviation convention of 'S' for the original samples. According to Fig. 6, The thermal conductivity of all samples after remaking showed a slight increase, within 3% of the initial value measured before unsealing the VIPs. It was concluded that all samples (S1, S2, S3 and S4) were reusable with a minimal impact on VIP thermal performance providing environmental and economic benefits.

3.4. Energy consumption of CPB over 10 years

The average duration of a typical curing and drying operation (4 h) was taken from commercial operators and this information was

Table 6
Time required for the tested VIPs to increase their thermal conductivity by 5 mW m^{-1} K^{-1} and 17 mW m^{-1} K^{-1} at 70 °C and 75 % RH.

Sample	Time (years) to increase by	
	5 mW m^{-1} K^{-1}	17 mW m^{-1} K^{-1}
S1	5.7	19.4
S2	1.7	5.9
S3	1.9	6.6
S4	4.6	15.5

used to calculate the cumulative energy consumption of a CPB over one year of operation (252 working days). VIP samples described previously and the ageing effect of on their thermal conductivity was accounted for. The VIP ageing behaviour is modelled using Equation (1) in Section 3.2, while Appendix B details the CPB energy simulation that applies the aged thermal conductivity values. No ageing was considered in the case of EPS. All findings are provided in Table 7. For VIPs reaching the envelope failure criterion before 10 years (Table 6), thermal conductivity beyond the failure point was conservatively taken as the measured atmospheric-pressure value.

The effect of varying thermal conductivities of VIPs on the total energy consumed in the first year and cumulatively over ten years is evident from Table 7. In the first year, the CPB insulated with S2 and S3 exhibited lower energy consumption than that insulated with S1. However, due to degassing, as explained in Section 3.2, the thermal conductivity of S2 and S3 increased over time and eventually became higher than that of S1 (after 2 years of operation). Consequently, over a decade of operation, the total energy consumption of the CPB insulated with S1 was lower than that of S2 and S3. Clearly, insulation thermal conductivity is the most critical factor influencing energy consumption compared to other factors such as climatic conditions, see Appendix C. It should be noted that the CPB model is intended for comparative analysis under identical conditions, and the reported absolute energy values should be interpreted as indicative rather than predictive of real industrial performance.

3.5. Interpretation of the LCA results

Cradle-to-gate, cradle-to-grave and cradle-to-cradle LCAs have been performed. VIPs with pristine core materials, TNF1, TNF2, and TNA, were used as references in the cradle-to-gate and cradle-to-grave phases. However, in the cradle-to-cradle phase, it was crucial to reflect real-life scenarios where energy consumption by the appliances/processes during usage-phase is significant. Therefore, VIPs with TNF1, TNF2, or TNA cores were excluded from this phase, as their thermal conductivity was not assessed due to the difficulty of producing 100% VIPs with these core materials.

3.5.1. Cradle-to-gate

All TNF materials (TNF1, TNF2 and TNA) were sourced from the same waste stream and processed within the same manufacturing facility. Therefore, it is reasonable to assume that they would exhibit similar environmental impacts in cradle-to-gate LCA. The primary distinction among these materials lies in TNA, which was partially pyrolysed. Conversely, FS followed a different processing route whilst the transportation distance from the mining site to the FS manufacturing facility was assumed to be same as that for TNF. The results of core LCA (cradle-to-gate) are presented in Table 8.

For all TNF materials, transportation (1 and 2), initial processing and packaging (raw material and processed material) accounted respectively for 67%, 26% and 3% of the total non-renewable energy impact. Due to different amounts and sources of energy (diesel or grid power) used climate change impact for TNA came from pyrolysis (67%) and transportation (30%).

In contrast, for FS, the industrial manufacturing accounted for 83% of the total non-renewable energy impact, whereas transportation contributed only 13%. When comparing all processed TNF materials with FS, the total non-renewable and renewable energy impacts for FS were found to be 7.2 times higher than those for TNF materials. However, such findings can be misleading. Many researchers might assume that the high energy consumption associated with FS processing accurately reflects its environmental impact. However, a crucial factor that must be considered is the quantity of material produced and transported relative to the energy consumed. This leads to the importance of defining a pertinent functional unit (FU) for LCA processes. For a 6.2-tonne raw material, production process yielded 2.1 tonnes of final FS product, whereas TNF1, TNF2, and TNA production resulted in 1.7 tonnes, 0.7 tonnes, and 0.2 tonnes of the final useable products, respectively. If an LCA study only considers the size of the VIP without standardising the raw material input (functional unit), the results will be invariably misleading. The actual environmental impacts of the core materials, presented in Table 9, were determined by using the core LCA results as input for the VIP LCA, which also compares the core material impacts with other components such as envelope, fleece, and different manufacturing process such as vacuuming, drying, testing, transportation and packaging of VIPs.

The VIP LCA confirmed the significance of transportation and raw material quantity in determining the environmental impact of VIPs. The combined non-renewable and renewable energy impact of FS was found to be 8.5 times higher than TNF1, 3.4 times higher than TNF2, and 1.03 times higher than TNA. While all other impacts were lower for TNF materials compared to FS, TNA exhibited higher climate change and acidification impacts, 2.7 times and 1.4 times greater, respectively, due to the amount and nature of the energy consumed in the pyrolysis process and emission from it.

Regarding the core material's contribution to total non-renewable and renewable energy impacts TNF1 accounted for 21%, TNF2 for 39%, FS for 67%, and TNA for the highest share at 69%. Transportation had the largest contribution to TNF1's total non-renewable and renewable impact (53%), followed by the envelope (19%), with the remaining 7% distributed across the other remaining

Table 7
Total energy consumption of CPB for VIP and EPS over 1 and 10 years (GJ).

	VIP				EPS
	S1	S2	S3	S4	
Total energy consumption of CPB in the 1st year (GJ)	43.3	42.7	42.8	42.5	55.1
Total energy consumption of CPB over 10 years (GJ)	440	454	451	434	551

Table 8
Impact categories results of the cradle-to-gate of the core LCA.

Impact categories	Transport 1 & 2		Packing		Processing	
	FS	TNF	FS	TNF	FS	TNF
Acidification (mol H^+ eq)	5.3	5.3	2.4	0.5	33.9	1.8
Climate Change (kg CO2 eq)	903.9	903.2	421.9	82.0	5988.8	2028.5
Non-Renewable (MJ)	16019.8	16019.8	8645.6	1696.9	122722.0	6245.5
Renewable (MJ)	53.9	53.9	197.2	637.1	56158.7	3494.5

Table 9
Impact categories results of the cradle-to-gate analysis of the VIP LCA.

Impact categories	FS	TNF1	TNF2	TNA	Other components
Acidification (mol H^+ eq)	0.07	0.02	0.04	0.1	0.07
Climate Change (kg CO2 eq)	18.4	2.7	6.8	49.6	11.8
Non-Renewable (MJ)	377.9	56.1	139.9	439.2	216.6
Renewable (MJ)	149.1	5.6	12.7	71.4	16.9

*Other components include vacuuming, drying and testing of the core materials, in addition to the transportation and packaging of one VIP.

components. Among these, core material drying contributed more than 70% of the remaining impact. The renewable energy attributed to 'Other components' is dominated by envelope production (46%), followed by drying (28%), testing (14%) and vacuuming (6%), with only minor contributions from packing, transport and fleece.

3.5.2. *Cradle-to-grave*

In this scenario, both the installation and end-of-life disposal of VIPs were considered. Installation required 200 g of polyurethane adhesive per VIP, a value assumed on standard bonding needs for rigid insulation panels in industrial settings. VIPs were assumed to be removed after 10 years, corresponding to the typical operational lifespan of a CPB, and transported 500 miles to a landfill site, representing a realistic long-distance disposal scenario. No electricity consumption was accounted for during VIP demolition, as it was assumed that the panels could be manually dismantled into core, fleece, and envelope components. This assumption was made due to the absence of reliable literature or accessible data quantifying energy requirements for VIP deconstruction or demolition at end-of-life. The only energy consumed in producing fertiliser bags to package and compress the cores was considered. Disposal data for fleece and envelope was sourced from SimaPro database, which showed an energy consumption of 0.2 MJ for 128 VIPs. Operational energy consumption in CPB was excluded from the cradle-to-grave evaluation to focus on raw material degradation.

Land use impact was included in the cradle-to-grave analysis and was quantified using landfill volume occupation of VIP cores at end-of-life as a proxy indicator.

Fig. 7 exhibited a comparable pattern to the cradle-to-gate results. S2 and S3 demonstrated the lowest embodied energy, indicating minimal renewable and non-renewable impact categories. Conversely, S4 displayed the largest non-renewable resource utilisation during production phase until the disposal (without accounting the CPB operational energy consumption), alongside the highest

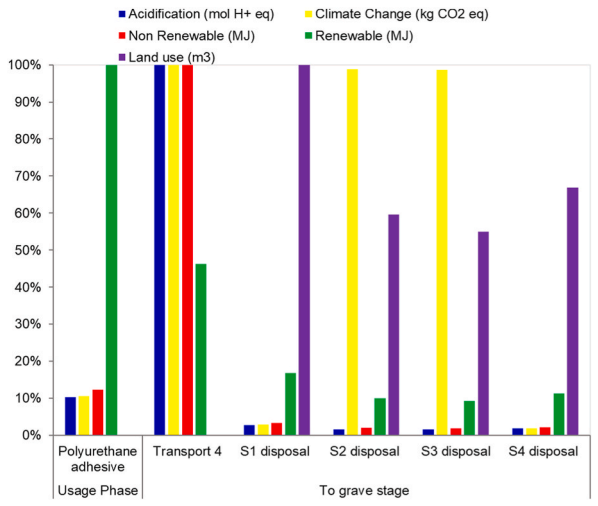

Fig. 7. Impact categories results of the usage phase, transportation and the disposal of four different core materials of VIPs in the cradle-to-grave scenario.

climate change impact, determined at 9087.77 kg CO_2 eq. However, unlike other materials, the disposal of S2 and S3 materials resulted in biological degradation, due to the presence of tree-based fibres, emitting both carbon dioxide and methane (CH_4) into the atmosphere, with no assumption of capture or repurposing for either gas. This degassing resulted in an increase of climate change impact by 3673.6 kg CO_2 eq for both TNF1 and TNF2 cores disposed, representing the highest contribution to climate change (cradle-to-grave), accounting for 54% and 50% of the total climate change impact value, respectively. The findings highlight the significant impact of material degradation in landfill sites on climate change, indicating that TNF waste should be reused instead of being dumped and ignored.

Despite S1 having the highest embodied energy, their climate impact was the lowest due to reliance on renewable energy and lack of degradation emissions. Thus, S1 were identified as the most environmentally sustainable option, see Fig. 7.

3.5.3. Cradle-to-cradle

LCA analyses was further extended to include transportation of VIPs from the CPB site (after its first useful life ended) to the manufacturing facility and reprocessing/remanufacture of VIPs. Materials such as polyethylene adhesive used to manufacture VIPs were considered at this stage. These changes increased the renewable impact, non-renewable impact, acidification, and climate change impact by 212.8 MJ, 22,483.3 MJ, 7.3 mol H^+ eq, and 1256.6 kg CO_2 eq, respectively, for all VIPs used in one CPB. The full life cycle energy consumption, including raw material extraction and usage phase was assessed, as shown in Table 10.

Using S1 (FS) as the reference baseline, the trade-off between energy demand and climate change impact was evaluated under the Cut-off approach. Relative to S1, S4 exhibited a lower total cradle-to-cradle energy demand despite higher electricity use, resulting in a reduction of 82,761 MJ in combined non-renewable and renewable energy over ten years of CPB operation compared to S1, see Table 10. This reduction reflects both lower operational energy consumption in the CPB and differences in embodied energy between the systems. However, these energy savings did not translate into a climate benefit. Compared with the baseline, the climate change impact of S4 remained 893 kg CO_2 eq higher, primarily due to emissions associated with the pyrolysis process used to produce TNA. A sensitivity analysis of the pyrolysis-related emissions is provided in Appendix C.

In contrast, S2 and S3 showed slightly lower climate change impacts than S1 (by 116 kg CO_2 eq and 104 kg CO_2 eq, respectively), but required higher total energy, exceeding the baseline by 18,904 MJ for S2 and 14,540 MJ for S3. When jointly considering energy demand and climate change performance relative to the baseline, S1 represents the most balanced "green core" option under the Cut-off approach, as illustrated in Fig. 8.

3.6. Reuse of core materials

As described in section 3.3, samples S2, S3, and S4 were found to be suitable for reusing as core materials for new VIPs. Reuse process requires core material transported from CPB site to VIP manufacturing facility and cores reused following process described in section 3.5.1.

Fig. 9 compares S1 and S2, showing reductions in environmental impacts when reuse is considered. S1 saw a 64% decrease in all impacts, except for renewable impact, which dropped 91% due to transportation's higher non-renewable burden. S2 and S3 impacts fell by 57% and 59%, with an 88% reduction in renewable impact. S4 showed the highest climate change reduction (74%) due to material degradation during initial preparation.

These results highlight the environmental benefits of reusing FS and TNA cores due to their higher embodied energy and CO_2 emissions. Clearly, reusability reduces energy consumption, carbon footprint, and environmental burden enabling a more sustainable production model.

3.7. Sensitivity analysis

Section 3.5.3 presented a cradle-to-cradle LCA of VIP composites using the cut-off approach with modified IEA 2022 data. This study underscores the importance of using updated data, selecting appropriate LCA methods, and understanding their impact on environmental assessments. The results detailed in section 3.5.3 were compared with those from Simapro without data adjustments and with the APOS approach, where data was modified in accordance with the same scope of work. Table 11 shows that S4 had the highest climate change impact when using cut-off approach (without modification) due to material degradation during pyrolysis, while S2 exhibited the highest acidification, non-renewable, and renewable impacts due to high energy consumption in the CPB. Non-renewable impact rose by 24% for all VIPs, while renewable impact dropped by 69%, leading to a 43% increase in climate change impact and a 4% rise in acidification (modified Cut-off approach). The modifications in this study reflect current UK data, consistent with the 2050 targets, whereas the unmodified data from SimaPro do not conform to these targets. While the results from SimaPro

Table 10
Results of various environmental impacts associated with distinct core materials in the cradle-to-cradle (Cut-off) scenario.

	S1	S2	S3	S4
Acidification (mol H^+ eq)	149	150	150	147
Climate Change (kg CO_2 eq)	26,615	26,499	26,511	27,508
Non-Renewable (MJ)	837,218	848,439	846,622	829,564
Renewable (MJ)	434,742	442,425	439,878	426,157

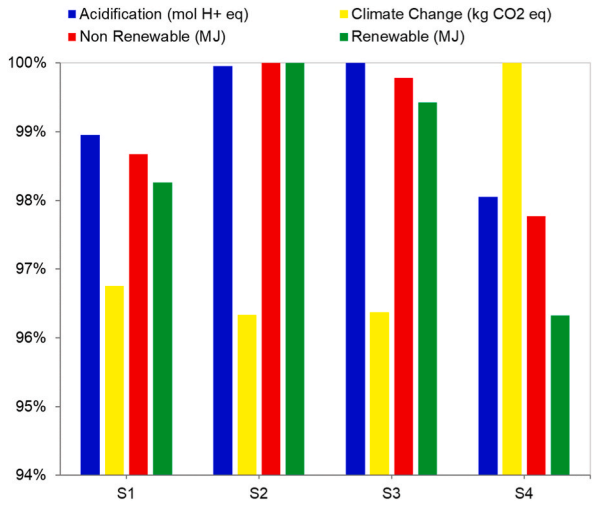

Fig. 8. Environmental impact and total impact of the four different VIP cores studied using Cut-off approach.

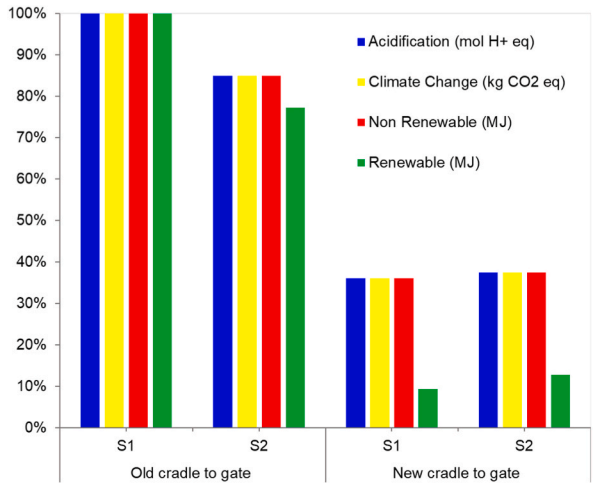

Fig. 9. Impact categories results comparing the original cradle-to-gate impacts with those when core is reused.

Table 11
Cradle-to-cradle impact categories results of various environmental impacts associated with core materials studied.

	Impact categories	S1	S2	S3	S4
Cut-off (SimaPro)	Acidification (mol H^+ eq)	154	158	158	153
	Climate Change (kg CO_2 eq)	46,576	46,301	46,328	47,235
	Non-Renewable (MJ)	1,103,532	1,119,995	1,116,526	1,091,122
	Renewable (MJ)	257,603	262,559	261090	252,827
APOS	Acidification (mol H^+ eq)	149	151	151	147
	Climate Change (kg CO_2 eq)	28,351	28,012	28,081	28,210
	Non-Renewable (MJ)	885,822	898,430	896,291	877,627
	Renewable (MJ)	457,833	465,937	463,249	448,812

(without modification) aid material selection process, they may obscure the true environmental benefits and implications of these products.

Under the APOS approach, S1 (FS) was also used as the reference baseline to evaluate the trade-off between energy demand and climate change impact. Unlike the Cut-off approach, APOS assigns avoided-burden credits to waste-derived TNF by accounting for the CO_2 and CH_4 emissions that would otherwise arise from biological degradation if the material were not utilised. In contrast, pyrolysis-related energy demand and direct gaseous emissions associated with TNA production are included as burdens in both modelling approaches.

Relative to the S1 baseline, S4 exhibited a lower total cradle-to-cradle energy demand, with a reduction of 17,216 MJ in combined non-renewable and renewable energy. In addition, S4 showed a lower climate change impact than S1 by 141 kg CO_2 eq, reflecting the combined effect of reduced CPB operational energy consumption and avoided emissions associated with the utilisation of TNF under APOS. This contrasts with the Cut-off interpretation, where end-of-life emissions dominate the climate change profile of S4.

S2 and S3 also exhibited lower climate change impacts than S1 under APOS (by 339 kg CO_2 eq and 270 kg CO_2 eq, respectively), but required higher total energy, exceeding the baseline by 20,712 MJ for S2 and 15,885 MJ for S3. Results further indicate that S2 retained the highest acidification, non-renewable, and renewable energy impacts, while S4 showed the lowest total energy demand see Table 11 and Fig. 10). When jointly considering energy demand and climate change performance relative to the baseline under APOS, S4 emerges as the preferred option, benefiting simultaneously from operational energy savings and avoided biomass degradation emissions.

This divergence arises from the treatment of biomass: APOS accounts for the avoided CO_2 and CH_4 emissions associated with the biological degradation of unused TNF, introducing a negative (credit) term for waste utilisation. Because S4 incorporates the greatest amount of TNF and exhibits the lowest CPB energy demand, it benefits simultaneously from reduced electricity consumption and avoided degradation emissions under APOS, leading to a lower climate change impact relative to the Cut-off results.

To provide a clearer comparison, the energy–climate trade-off was expressed as the amount of climate change impact per unit of operational energy saved, calculated as kg CO_2 eq per GJ of energy saved relative to, the reference baseline, S1(FS). Under the Cut-off scenario used in this study, S4 resulted in approximately 55.0 kg CO_2 eq per GJ of energy saved, indicating a climate penalty for the achieved energy savings. Under the Cut-off (SimaPro) scenario, S4 resulted in approximately 38.3 kg CO_2 eq per GJ of energy saved relative to S1, again indicating a climate penalty associated with the energy savings. In contrast, under the APOS scenario, S4 achieved approximately (−) 8.2 kg CO_2 eq per GJ of energy saved, reflecting simultaneous reductions in both energy demand and climate impact. This indicator is only applicable to systems that achieve a net reduction in total energy demand relative to the reference; therefore, it was not calculated for S2 and S3, which exhibit higher energy consumption than S1.

3.8. Prediction of LCA of VIPs in 2050

The UK is committed to achieving a net-zero emission economy by 2050, which includes transitioning to a fully decarbonised electricity grid and transport sector. To evaluate the long-term sustainability of VIP core materials under this future scenario, both the Cut-off and APOS life cycle approaches were employed. In this scenario, transportation-related emissions were excluded based on the assumption that future freight will be powered by zero-carbon technologies such as electric batteries or hydrogen fuel cells. Only climate change impacts from raw material degradation such as pyrolysis of biomass-based cores were considered. The 2050 scenario represents a policy-aligned, normative case assuming full energy decarbonisation; material degradation pathways were kept unchanged, and APOS credits arise exclusively from avoided biomass decay rather than from modified future process efficiencies. S1 (FS) had the highest energy consumption in both approaches. S4, S3, and S2 had less embodied energy as already showed in previous sections, see Table 12.

S1 (FS VIP) had zero CO_2 emissions, but TNA materials released 1149.3 kg of CO_2 during pyrolysis. The APOS approach, which accounts for process interdependence and allocated environmental impacts based on each process's contribution to the overall system, highlighted S4 as the most environmentally beneficial, requiring 2742.9 kg of TNF waste for TNA production, followed by TNF1 (1745.5 kg) and TNF2 (685.71 kg) to produce 192 kg of materials (30% of the total 640 kg used for 128 VIPs).

The results from Cut-off and APOS approaches (Fig. 11a and b) demonstrate that APOS approach due to its ability to account for the effect of waste, in the case when the raw material is left to decay, will yield more realistic LCA results for VIPs using TNF as core

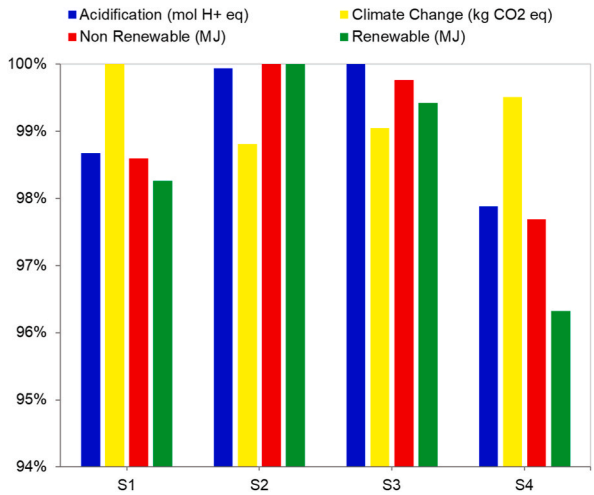

Fig. 10. APOS approach predicted environmental impact and total impact of the four different VIP cores studied.

Table 12
Climate change, embodied energy and total energy consumed (including CPB energy consumption) of four core materials using both Cut-off and APOS approaches.

	Environmental impacts	VIP Samples			
		S1	S2	S3	S4
Cut-off	Climate change (kg CO_2 eq)	0	0	0	1149
	Embodied energy (MJ)	119,537	101,501	105,028	118,732
	Total energy consumed (MJ)	1,271,959	1,290,864	1,286,499	1,255,720
APOS	Climate change (kg CO_2 eq)	0	−3940	−10,031	−15,763
	Embodied energy (MJ)	126,865	107,723	111,466	126,010
	Total energy consumed (MJ)	1,343,655	1,364,367	1,359,540	1,326,440

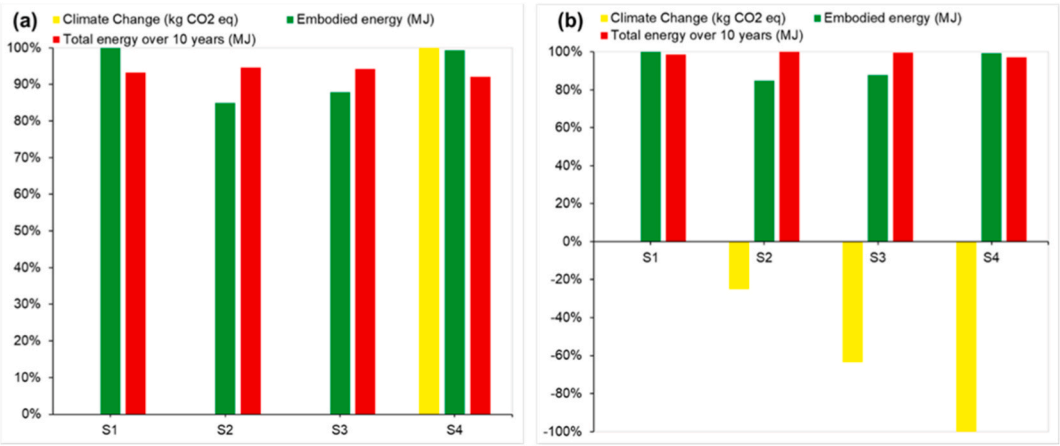

Fig. 11. Comparison of climate change and renewable impacts of four different core VIPs in year 2050 using both (a) Cut-off and (b) APOS approaches.

material. On using the TNF derived from tree waste, S4, is shown to reduce highest emissions by 15763 kg CO2 eq; see Table 12 and Fig. 11b.

4. Conclusions

The present study focused on the experimental thermophysical and environmental characterisation of fumed silica and three new core materials derived from tree-based natural fibre waste. The thermal conductivity of VIPs manufactured using optimised core compositions was measured at 20-70 °C and 0.64-1000 mbar. A system-scale model of a typical vehicle painting booth was developed using COMSOL Multiphysics and its energy consumption predicted. The findings of were used to perform a comprehensive LCA from 'cradle-to-gate' to 'cradle-to-cradle' basis. Methodologies, data and results presented here can be used by future designers and end-users to assess greenness of a given VIP. This study advances knowledge by applying life cycle assessment to high-temperature industrial applications, an area underrepresented in previous VIP research. It also introduces and experimentally validates a novel core material (FS-TNA), integrates reusability scenarios, and compares environmental outcomes using both Cut-off and APOS allocation models. These findings contribute to ongoing efforts to align insulation material innovation with decarbonisation policies and net-zero targets.

The main conclusions are as follows.

- S4 (FS–TNA, 70:30 wt%) exhibited the lowest thermal conductivity, measuring 6.23 mW $m^{-1}\cdot K^{-1}$ at 20 °C and 7.41 mW $m^{-1}\cdot K^{-1}$ at 70 °C, confirming superior insulation performance at elevated temperatures.
- FS–TNF1(FS–TNF1, 70:30 wt%) and FS–TNF2 (FS–TNF2, 70:30 wt%) showed faster ageing, with thermal conductivity exceeding that of FS after approximately two years, driven by fibre-related outgassing.
- Under the Cut-off approach and relative to S1, S4 reduced total cradle-to-cradle energy demand by 82,761 MJ over 10 years but showed a higher climate change impact of 893 kg CO_2 eq due to pyrolysis-related emissions.

- S2 and S3 showed slightly lower climate change impacts than S1 by 116 kg CO_2 eq and 104 kg CO_2 eq, respectively, but required higher total energy by 18,904 MJ and 14,540 MJ, respectively.
- Under the APOS approach, S4 achieved both lower total energy demand by 17,216 MJ and lower climate change impact by 141 kg CO_2 eq relative to S1.
- S2 and S3 also showed lower climate change impacts than S1 under APOS by 339 kg CO_2 eq and 270 kg CO_2 eq but required higher total energy by 20,712 MJ and 15,885 MJ, respectively.
- When expressed per unit of energy saved relative to S1, S4 resulted in 55.0 kg CO_2 eq per GJ under the modified Cut-off scenario used as the main model, 38.3 kg CO_2 eq per GJ under the unmodified Cut-off scenario from SimaPro used for comparison, and (−) 8.2 kg CO_2 eq per GJ under the modified APOS scenario used as an alternative allocation approach.
- Future work should focus on scaling FS–TNA VIP production, validating long-term in-field performance, and collaborating with industry to benchmark CPB energy models against operational data, thereby supporting deployment of advanced insulation materials aligned with decarbonisation and net-zero targets.
- Future work should explicitly account for upstream fumed silica production losses, including dust generation and associated emission control energy, which were outside the scope of the present study due to limited publicly available data.
- Further LCA scenarios should also explore alternative electricity grid mixes beyond the UK, as VIP and core material manufacturing often occurs in regions with substantially different energy mixes, which may significantly influence comparative environmental performance.

Overall, FS VIPs represent the most balanced and low-risk option under the Cut-off approach, while FS–TNA VIPs show improved performance under the APOS scenario due to combined operational energy savings and circular-economy assumptions. These APOS-based outcomes are conditional on modelling choices related to avoided biomass degradation and allocation and should therefore be interpreted as scenario-dependent rather than deterministic indicators of material performance. These findings demonstrate that VIP selection for high-temperature industrial applications must account for ageing, operational energy, and allocation methodology rather than thermal performance alone.

CRediT authorship contribution statement

Tarek Raad: Writing – original draft, Visualization, Validation, Software, Methodology, Investigation, Formal analysis, Data curation, Conceptualization. **Harjit Singh:** Writing – review & editing, Supervision, Resources, Methodology, Funding acquisition, Conceptualization. **Suresh Sivan:** Writing – review & editing, Project administration, Funding acquisition.

Declaration of competing interest

The authors declare that they have no known competing financial interests or personal relationships that could have appeared to influence the work reported in this paper.

Acknowledgment

Singh and Sivan thankfully acknowledge India's SPARC 2019-2020 funding received for the project number 2066.

Appendix A

Materials

Tree based natural materials were processed into two distinct fibres of varying sizes, which were then used to create composites with fumed silica [37]. Commercially available aluminium coated polyethylene film (Avery Dennison) was used as barrier.

The natural fibres underwent a cleaning process use distilled water to eliminate any collected dust particles. Subsequently, the TNF underwent a drying process in an oven maintained at 60 °C for 24 h, was ground with a mechanical grinder, and was sieved through two distinct mesh sizes to get a specific grade as illustrated in Fig. A. 1. Two distinct fibres, TNF1 and TNF2, were generated, displaying average fibre lengths of 0.82 mm and 0.22 mm, respectively. The remaining sieved tree-based materials were deemed unsuitable as core materials for VIP and were subsequently pyrolysed into Tree-based Natural Ash (TNA) at a specified temperature to optimise the utilisation of tree-based waste, as illustrated in Fig. A. 2.

The composite samples were further compacted to produce cores measuring 150 mm × 150 mm. Subsequently, the core samples were dried in a vacuum oven to minimise moisture content. These cores were used to manufacture VIPs using an in-house vacuum sealer equipment.

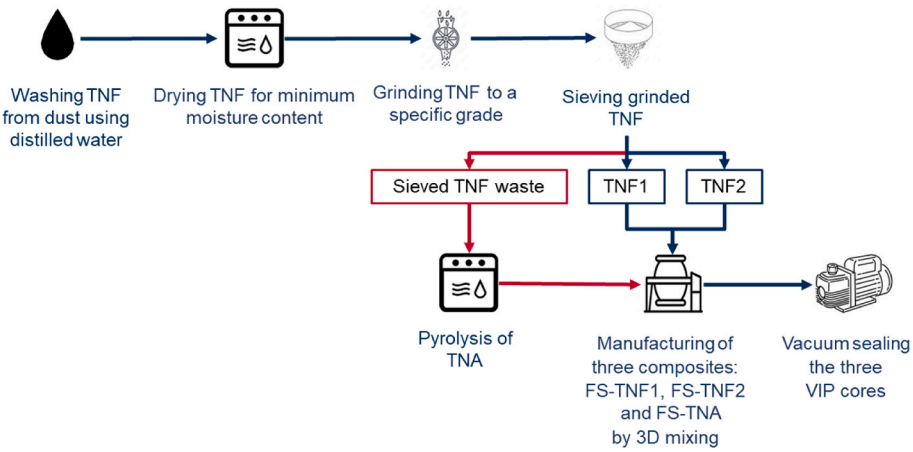

Fig. A. 1. Production of TNF1, TNF2, TNA and composites employed in this study.

Table A. 1
Average pore diameter, porosity and bulk density comparison of studied samples

Sample	Total intrusion volume x 10^{-6} (m^3g^{-1})	Total pore area (m^2g^{-1})	Average pore diameter x 10^{-6} (m)	Porosity (%)	Bulk Density (kgm^{-3})
S1	17.41	264.24	0.26	91.54	52.60
S2	10.01	170.74	0.23	88.27	88.20
S3	9.33	189.32	0.19	89.44	95.80
S4	11.24	234.61	0.19	88.37	78.60

The average pore diameter, porosity, and bulk density of the studied samples, obtained using Mercury Intrusion Porosimetry (MIP), are presented in Table A.1. Scanning Electron Microscopy (SEM) images of the bonding structure of the samples are shown in Fig. A. 2.

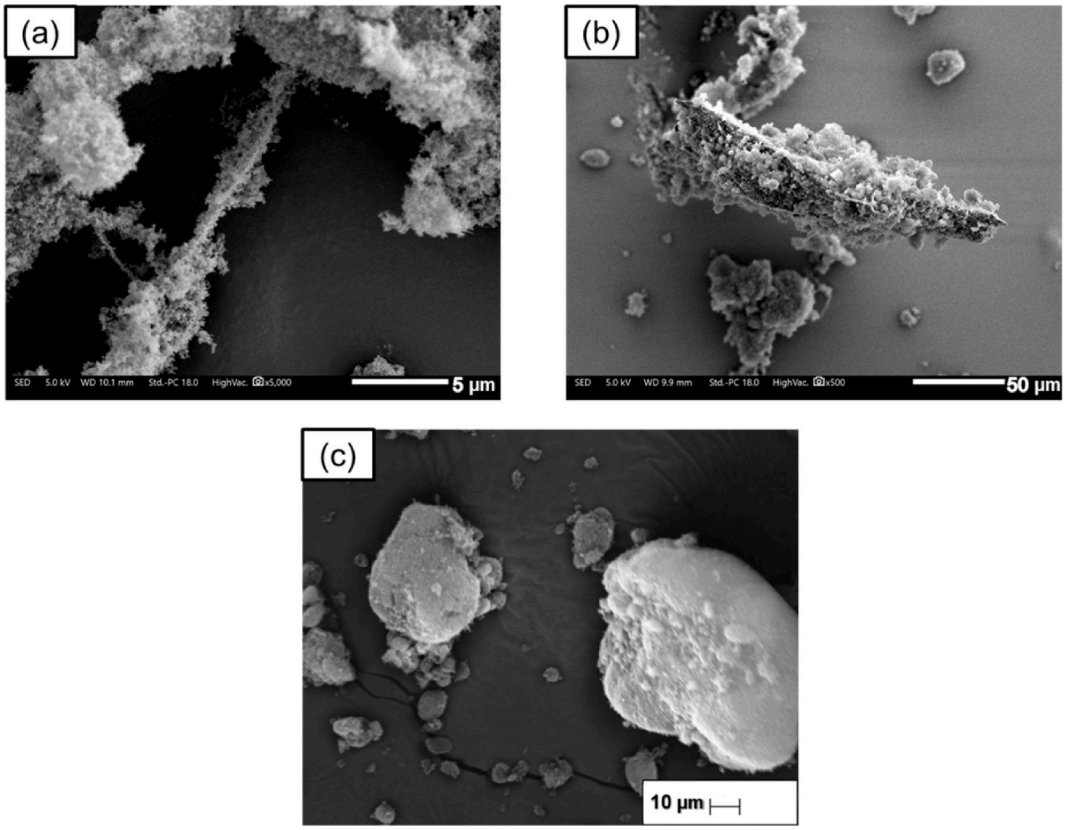

Fig. A. 2. SEM images of (a) S2, (b) S3 and(c) S4.

Measurement uncertainty

The heat flow meter (NETZSCH HFM 446 Lambda) has thermocouples located in each plate, along with a heat flux sensor situated at the centre of the plate. This arrangement allowed for the determination of the overall thermal conductivity at the centre of the panel of VIP. The calculation of the thermal conductivity was based on Fourier's law, as depicted in Equation (A1). The law of propagation of errors was employed to determine the level of uncertainty associated with the thermal conductivity measurements as presented in Equation (A2).

$$\lambda = \frac{q\Delta d}{\Delta T} \tag{A1}$$

$$\left(\frac{\partial\lambda}{\lambda}\right)^2 = \left(\frac{\partial q}{q}\right)^2 + \left(\frac{\partial\Delta d}{\Delta d}\right)^2 + \left(\frac{\partial\Delta T}{\Delta T}\right)^2 \tag{A2}$$

where λ is thermal conductivity value, q heat flux, d thickness of the VIP and ΔT difference in temperature.

VIP thickness was measured with a minimum accuracy of 0.001 mm, while the temperature was determined with a minimum accuracy of 0.1 K. As a result, the individual uncertainty associated with these measurements was exceptionally minimal. Due to that, the uncertainty in the thermal conductivity readings was attributed to the accuracy of the heat flux measurement. Specifically, for the HFM 446 Lambda, the accuracy ranged from a minimum of 1% to a maximum of 3%. The HFM was calibrated prior to testing using the calibration procedure outlined in Section 8.6 of ASTM C1667–15, ensuring stable and reliable thermal conductivity measurements throughout the experimental programme.

Appendix B

Example application

This study investigates high-temperature applications, specifically up to 70 °C. Accordingly, a car painting booth (CPB) was selected as a representative case to assess the energy consumption associated with various VIPs core materials. CPBs are controlled environments designed to enhance paint quality by managing airflow and temperature. They are classified into cross-draft, downdraft, and semi-downdraft types. Cross-draft booths, the most widely used due to their affordability, direct airflow horizontally and was selected for this study.

A three-dimensional finite element model of a cross-draft CPB was developed in COMSOL Multiphysics, see Fig. B. 1a. The booth, comprising a ceiling, floor, and four structural walls, was designed based on standard market dimensions and the selected car size, see Table B. 1. Four sensors were positioned above the steel car to regulate heating, see Fig. B. 1b. The walls were insulated with various materials, primarily Expanded Polystyrene (EPS), which is commonly used in CPBs with a typical thickness of 75 mm. To assess the feasibility of replacing conventional insulation with VIPs, a comparison was conducted between EPS and VIPs at a fixed thickness of 25 mm. VIPs with a thickness of 25 mm were analysed using different core materials, namely S1 (FS), S2 (FS–TNF1), S3 (FS–TNF2), and S4 (FS–TNA).

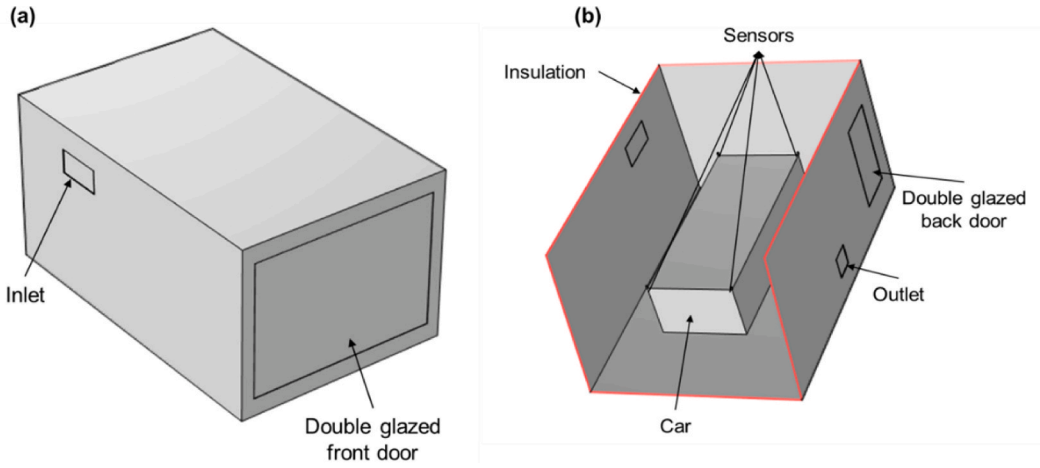

Fig. B. 1. (a) Three-dimensional view and (b) internal view of the CPB studied.

Table B. 1
Geometric parameters of the CPB components

Description	Value	Unit
Wall length	6.9	m
Wall width	4.5	m
Wall height	3.5	m
Insulation thickness	25	mm
Inlet area	0.5	m^2
Outlet area	0.25	m^2
Double-glazed glass front door area	9.6	m^2
Double-glazed glass back door area	2	m^2
Car length	4.5	m
Car width	1.8	m
Car height	1.2	m
Sensor volume	27	cm^3

The model integrates turbulent flow and heat transfer in solids and fluids. The k-ω turbulence model was chosen for its accuracy in capturing near-wall effects, ensuring reliable airflow simulations [38]. Heat transfer was modelled through conduction, convection, and surface-to-surface radiation to assess temperature distribution. The heat transfer phenomena in solids and fluids are described by Equation (B1) and Equation (B2).

$$\rho C_p \frac{\partial T}{\partial t} + \rho C_p u.\nabla T + \nabla.q = Q \tag{B1}$$

$$q = -k\nabla T \tag{B2}$$

where ρ is the material density, C_p the material specific heat, u the velocity field, T the temperature field, t the time, q the heat flux, Q the heat energy and k thermal conductivity.

The booth was assumed to operate at ambient UK temperatures, with seasonal variations considered. A heating system (20 kW) controlled the inlet air temperature to maintain a setpoint of 70 °C. Air entered the booth at 0.4 m/s, ensuring uniform temperature distribution [39]. The sensors monitored the booth's temperature, automatically stopping the hot air flow once the average temperature reached 70 °C. This approach was essential for evaluating the energy efficiency of different insulation types used in the CPB. The inlet air temperature was calculated using the energy balance Equation (B3), ensuring efficient heating system operation by maintaining the paint application process and supplying heat only when necessary.

$$T_{in} = T_{out} + \left(\frac{P_{heater} \cdot step1(T_C)}{\dot{m} \cdot C_p} \right) \tag{B3}$$

where, T_{in} is the inlet temperature of the air, T_{out} the outlet temperature, P_{heater} the heater power, $\dot{m}$ the mass flow rate of the air and C_p the average specific heat capacity of the air within the system, outlet and T_C the sensor temperature.

C_p was determined by considering the conditions at the outlet, which accurately represents the temperature state of the air as it exits the system. The calculation of this mean value was crucial in determining the amount of energy that was transported by the air. The function $step1(T_C)$ serves as a binary control that turns on or off the heater depending on the temperature reading from the employed sensors. When T_C is lower than the T_{set}, the function has a value of 1, indicating that the heater is activated, and energy is consumed. Once T_C reaches or surpasses T_{set}, the function value becomes equal to 0, causing the heater to turn off and no energy consumption to occur. The incorporation of this boundary condition and temperature control guarantees a more effective energy system for the car painting booth.

This study did not consider any potential leakage of air and heat through door gaskets.

Sensitivity analysis

To verify the accuracy and reliability of the car painting both model, two sensitivity analyses were performed. The first study concentrated on mesh size, whereas the second investigated the impact of time step selection. Due to the significance of accurate temperature data recording in the model, especially from the small sensors located within the booth, the mesh size of the sensors was determined to be finer than that of the overall CPB. The decision was made because the sensors, being considerably smaller than the booth, necessitate a higher resolution mesh to accurately capture localised thermal gradients. A free tetrahedral mesh was utilised, with the sensor mesh consistently one size smaller than that of the CPB. Five mesh configurations were evaluated: Coarser + Coarse (25,186 elements), Coarse + Normal (45,059 elements), Normal + Fine (95,251 elements), Fine + Finer (265,482 elements), and Finer + Extra Fine (1,897,645 elements). An EPS insulation with a thickness of 25 mm was utilised at an ambient temperature of 6.3 °C for all varying mesh sizes.

The findings in Fig. B. 2 revealed that the energy consumption for the largest mesh was 255.27 MJ, whereas the energy consumption using the smallest mesh was 249.36 MJ, resulting in a difference of approximately 2.3%. As anticipated, finer meshes offered more precise energy consumption estimates, accurately reflecting intricate thermal gradients, particularly in regions with complex geometries. Nonetheless, the mesh 3 (Normal + Fine) showed results that were approximately 0.2% superior to those obtained from

the finest mesh (Finer + Extra Fine). Mesh 3 provides an optimal equilibrium between computational efficiency and precision, with energy consumption variations staying within acceptable thresholds relative to the coarser meshes. Thus, the Normal mesh for the CPB and the Fine mesh for the sensors were identified as the optimal configuration for the model.

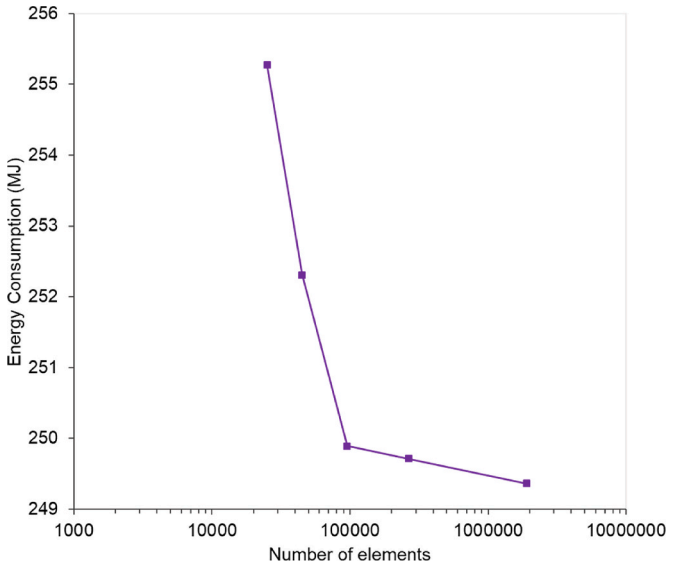

Fig. B. 2. Mesh independence study for CPB insulated with EPS (25 mm) at 6.3 °C using 5 different mesh scenarios.

In the second sensitivity analysis, four distinct time steps of 5, 10, 15, and 20 s were selected to investigate their effect on the energy consumption of the CPB. The identical EPS with a thickness of 25 mm at an ambient temperature of 6.3 °C was selected.

Table B. 2
Total energy consumption of CPB insulated with 25 mm EPS at different time steps

Time Step (s)	Operational Time (s)	Total Energy Consumption (MJ)
5	14265	249.61
10	14270	249.89
15	14270	250.13
20	14270	250.21

The results displayed in Table B. 2 indicated that the operational duration for CPB was identical across all selected time steps, except for the 5-s time step, which recorded a total operational time of 14,265 s, representing a reduction of 5 s. However, regarding total energy consumption, a minor variation not exceeding 0.6 MJ was observed between the shortest time step (5 s) and the longest time step (20 s). Utilising a smaller time step, such as 5 s, facilitates a more detailed monitoring of temperature variations within the booth, thereby enhancing the accuracy and precision of the simulation. However, in this case, a larger time step exhibited minimal errors in energy consumption estimates. A 10-s time step was selected as it offered an optimal equilibrium between accuracy, computational efficiency, and simulation duration.

Appendix C

Additional changes in the system model

SimaPro offers three choices for road transport: small trucks (less than 10 tonnes) with an average load capacity of 3 tonnes, medium-sized vehicles (10-20 tonnes) with an average load capacity of 6.2 tonnes and large trucks (above 20 tonnes) with an average load capacity of 24 tonnes. Emissions were assessed based on truck types, fuel consumption, and load conditions. The emission factor for CO_2 was 2.64 kg CO_2 per liter of fuel [40]. SimaPro faced challenges in controlling fuel usage and distance separately, as the model only provided specific load factors (20%, 50%, 80%, 100%). Additionally, SimaPro's truck model supports only up to EURO5 emission standards, but the European Commission proposed a new EURO7 standard in 2022.

Modifications were needed to develop a customised method due to real-world discrepancies. Fuel consumption per unit distance remained consistent, but emissions per tonne-kilometre (tkm) increased with distance. The Mercedes Benz Actros L [41] was selected as a representative model. The fuel consumption of this vehicle ranges from 25 to 35 L per 100 km, depending on factors such as road conditions and the amount of load it carries. The truck was estimated to consume 35 L per 100 km when driving in urban areas, 30 L on country roads, and 25 L on highways when carrying a load. When the vehicle was empty, it was projected to consume 25 L per 100 km

on all three types of roads. The newly introduced impact categories, specifically climate change and acidification, are displayed in Table C. 1.

Table C. 1
The new impact categories based on the load of the truck of different materials

Truck loading different materials	Load (tonnes)	Emission per tkm (kg CO_2 eq)	Climate change (kg CO_2 eq)	Acidification (mol H^+ eq)
Silicon tetrachloride	5.92	1.46	59.82	0.43
TNF waste	6.15	1.41	59.77	0.43
TNF processed	2.64	3.27	61.64	0.43
FS	2.19	3.95	62.31	0.43
VIPs	0.64	13.52	159.43	1.07

The Land use impact category utilising EN15804+ A2 was excluded because of its intricate nature and lack of assurance. The only assumption used was to calculate the emissions of gases, such as CO_2 and CH_4, during the degradation of TNF, based on its chemical composition. Additionally, the area of land required for the disposal of materials, such as FS, was determined based on the quantity and density of the material.

TNF mostly contains cellulose, hemicellulose and lignin. The degradation of these molecules occurs primarily through anaerobic microbial degradation over time [42]. The decomposition of cellulose and hemicellulose takes place according to Equations (C1) and (C2) respectively.

$$(C_6H_{10}O_5)n + nH_2O \rightarrow 3nCO_2 + 3nCH_4 \quad \text{(C1)}$$

$$(C_5H_8O_4)n + nH_2O \rightarrow 2.5nCO_2 + 2.5nCH_4 \quad \text{(C2)}$$

One kg of sample would be decomposed to 491 g of carbon dioxide and 178.8 g of methane which was due to the decomposition of cellulose and hemicellulose. Lignin is more resistant unlike cellulose or hemicellulose towards degradation. It decomposes very slowly but eventually forms humic substances and landfill gases.

Upon analysing the IEA collected data, it was seen that the primary sources of energy generation in the year 2016 and according to the most recent data provided in 2022 are displayed in Table C. 2 together with their respective contributions to the total electricity generation.

Table C. 2
Difference in electricity generation sources in the UK between 2016 and 2022

Electricity generation sources in UK	Value (GWh) year 2016	% Year 2016	Value (GWh) year 2022	% Year 2022
COAL	31,435	9.3	7066	2.2
OIL	1890	0.6	2097	0.7
GAS	143,356	42.5	125,300	38.7
NUCLEAR	71,726	21.3	47,723	14.7
HYDRO	8329	2.5	7307	2.3
TIDE	0	0	9	2.8E-03
BIOFULES	27,325	8.1	30,666	9.5
WASTE	5628	1.7	9655	2.9
WIND	37,159	11.0	80,162	24.8
SOLAR	10,395	3.1	13,920	4.3
Total SOLAR, WIND	47,554	14.1	94,082	29.1
Total	337,243		323,905	

Table C. 2 revealed a significant shift in electricity generation sources in the UK between 2016 and 2022. It is widely recognised that the UK is actively pursuing a strategy to achieve net zero emissions by 2050 [43]. When striving for more precise outcomes, it was crucial to adjust to the ongoing changes. The outcomes of the alternative methodology were displayed in Table C. 3and subsequently utilised in the study.

Table C. 3
New values of the impact category based on the IEA (2022) based on 1 MJ of electricity - Cut-off and APOS approaches

Impact category/*Substances*	SimaPro Value (MJ)		New Value based on IEA in 2022 (MJ)	
	Cut-Off	APOS	Cut-Off	APOS
Non-renewable, fossil	1.29	1.44	1.24	1.32
COAL	0.13	0.25	0.06	0.07
GAS	1.11	1.12	1.15	1.23
OIL	0.05	0.07	0.02	0.02
Peat	1.05E-03	1.19 E−03	-	-

(*continued on next page*)

Table C. 3 (*continued*)

Impact category/*Substances*	SimaPro Value (MJ)		New Value based on IEA in 2022 (MJ)	
	Cut-Off	APOS	Cut-Off	APOS
Non-renewable, nuclear	0.97	1.04	0.44	0.47
Non-renewable, biomass	2.02E-05	4.03E-05	-	-
Renewable, biomass	0.21	0.19	-	-
Renewable, wind, solar, geotherm	0.32	0.27	0.87	0.92
Renewable, water	0.03	0.03	0.07	0.07
TOTAL	2.82	2.98	2.61	2.78

Transport sensitivity analysis

A sensitivity analysis was conducted to assess the influence of transport distance on the life-cycle results. Fuel consumption and associated impacts were recalculated for four haul distances (100, 200, 500, and 1000 miles), considering both fully loaded transport and empty return trips. The resulting environmental indicators were then compared to the baseline case to evaluate how variations in transport assumptions affect the overall outcomes. This analysis allows isolation of the contribution of transport logistics to total impacts and tests the robustness of the comparative results across different distance scenarios, presented in Table C.4.

Table C. 4
Diesel fuel consumption for loaded and empty truck transport at different haul distances

Distance (miles)	Truck Loaded		Truck Empty		Total
	(L)	(kg)	(L)	(kg)	(kg)
100	44.83	38.11	40.23	34.20	72.31
200	89.66	76.21	80.47	68.39	144.6
500	224.14	190.52	201.17	170.99	361.51
1000	448.28	381.04	402.34	342.00	723.04

Table C.5 presents the cradle-to-cradle results for scenarios S1 and S2 under increasing transport distances (100, 200, 500, and 1000 miles). As expected, all impact categories rise with longer haul distances, reflecting the growing contribution of transport to the overall life-cycle inventory. Despite the higher absolute impacts at longer distances, the relative relationship between S1 and S2 remains consistent across all distances, indicating that the comparative conclusions of the study are robust to variations in transport assumptions.

Table C. 5
Cradle to cradle results using different haul distances

	100 miles		200 miles		500 miles		1000 miles	
	S1	S2	S1	S2	S1	S2	S1	S2
Acidification (mol H+ eq)	139	141	142	143	151	152	165	166
Climate Change (kg CO_2 eq)	24923	24845	25443	25327	27003	26770	29603	29177
Non Renewable (MJ)	802533	814548	813187	824409	845155	853996	898438	903309
Renewable (MJ)	434625	442311	434661	442344	434768	442444	434947	442610

Pyrolysis sensitivity analysis

A sensitivity analysis was performed to assess the influence of the pyrolysis sub-model on S4. The variation was applied only to the calculated pyrolysis-related emission Equations (C1) and (C2) and to the furnace energy used in S4, as these parameters were estimated rather than measured. Three scenarios were evaluated relative to the base case: (−) 30%, (−) 50%, and (+) 30%, representing reductions (−) and an increase (+) in the assumed pyrolysis-related emissions and energy demand. The results were compared with the reference baseline (S1), while all other model parameters were kept unchanged. Results are presented in Table C.6.

Table C. 6
Sensitivity of S4 results to variation in pyrolysis-related emissions

	S1	S4			
	Base study	Base study	(−) 30%	(−) 50%	(+) 30%
Acidification (mol H^+ eq)	149	147	147	146	148
Climate Change (kg CO_2 eq)	26615	27508	27130	26879	27885

(*continued on next page*)

Table C. 6 (*continued*)

	S1	S4			
	Base study	Base study	(−) 30%	(−) 50%	(+) 30%
Non Renewable (MJ)	837218	829564	828482	827760	830646
Renewable (MJ)	434741	426157	425551	425147	426762

Under the base-case Cut-off scenario, S4 showed a climate change impact of 27,508 kg CO_2 eq, compared with 26,615 kg CO_2 eq for S1 (FS), corresponding to a penalty of 893 kg CO_2 eq. At the same time, S4 reduced total energy demand by 16,239 MJ (16.24 GJ) relative to S1, corresponding to 55.0 kg CO_2 eq per GJ of energy saved. With a (−) 30% variation, the climate impact corresponded to 31.7 kg CO_2 eq per GJ of energy saved. Under the (−) 50% scenario, the value decreased to 16.3 kg CO_2 eq per GJ of energy saved. With a (+) 30% variation, the value increased to 78.2 kg CO_2 eq per GJ of energy saved. Across all scenarios, acidification changed only marginally (149–146 mol H^+ eq), reflecting its direct dependence on total energy demand, which varied only slightly. In contrast, climate change results were influenced by both energy demand and the CO_2 and CH_4 emissions, leading to moderate variations in the trade-off values. However, the pattern of the total energy saving of S4 relative to S1 remained essentially unchanged across all sensitivity scenarios, indicating that the primary energy advantage observed in the base case is not affected by reasonable variations in the pyrolysis-related assumptions. This confirms the robustness of the model within the tested uncertainty range.

Data availability

Data will be made available on request.

References

[1] DESNZ, Clean power 2030 action plan: a new era of clean electricity. www.gov.uk/desnz, 2024.
[2] K.A. Al-Sallal, Comparison between polystyrene and fiberglass roof insulation in warm and cold climates. www.elsevier.com/locate/renene, 2003.
[3] N.H. Ramli Sulong, S.A.S. Mustapa, M.K. Abdul Rashid, Application of expanded polystyrene (EPS) in buildings and constructions: a review, J. Appl. Polym. Sci. 136 (2019), https://doi.org/10.1002/app.47529.
[4] I. Gnip, S. Vejelis, S. Vaitkus, Thermal conductivity of expanded polystyrene (EPS) at 10 °c and its conversion to temperatures within interval from 0 to 50 °c, Energy Build. 52 (2012), https://doi.org/10.1016/j.enbuild.2012.05.029.
[5] EPBD, Energy Performance of Buildings Directive, Second Cost Optimal Assessment for the United Kingdom, 2019.
[6] DEFRA, Single-Use Plastics Bans and Restrictions, 2023.
[7] SMMT, Automotive sustainability report 2023 data. https://www.smmt.co.uk/wp-content/uploads/SMMT-Sustainability-25th-Report-2024.pdf, 2024. (Accessed 12 March 2024).
[8] P.P. Rao, A. Gopinath, Energy savings in automotive paint ovens: a new concept of shroud on the carriers, Journal of Manufacturing Science and Engineering, Transactions of the ASME 135 (2013) 1–9, https://doi.org/10.1115/1.4024537.
[9] X. Wang, N. Walliman, R. Ogden, C. Kendrick, VIP and their applications in buildings: a review, Proceedings of the Institution of Civil Engineers - Construction Materials 160 (2007) 145–153, https://doi.org/10.1680/coma.2007.160.4.145.
[10] M. Alam, M. Picco, S. Resalati, Comparative holistic assessment of using vacuum insulated panels for energy retrofit of office buildings, Build. Environ. 214 (2022), https://doi.org/10.1016/j.buildenv.2022.108934.
[11] S. Verma, H. Singh, Vacuum insulation in cold chain equipment: a review, in: Energy Procedia, Elsevier Ltd, 2019, pp. 232–241, https://doi.org/10.1016/j.egypro.2019.02.086.
[12] D. Kaushik, H. Singh, S.A. Tassou, Vacuum insulation panels for high-temperature applications – design principles, challenges and pathways, Therm. Sci. Eng. Prog. 48 (2024), https://doi.org/10.1016/j.tsep.2024.102415.
[13] M.R. Jalali, D. Kaushik, S. Verma, H. Singh, A coupled model of finite element method and Mie theory for heat transfer inside expanded perlite vacuum insulation panels (VIPs) at high temperatures, Int. J. Heat Mass Tran. 219 (2024), https://doi.org/10.1016/j.ijheatmasstransfer.2023.124885.
[14] M. Alam, H. Singh, M.C. Limbachiya, Vacuum insulation panels (vips) for building construction industry - a review of the contemporary developments and future directions, Appl. Energy 88 (2011) 3592–3602, https://doi.org/10.1016/j.apenergy.2011.04.040.
[15] P. Karami, N. Al-Ayish, K. Gudmundsson, A comparative study of the environmental impact of Swedish residential buildings with vacuum insulation panels, Energy Build. 109 (2015) 183–194, https://doi.org/10.1016/j.enbuild.2015.10.031.
[16] R.F. De Masi, A. Gigante, G.P. Vanoli, Are nZEB design solutions environmental sustainable? Sensitive analysis for building envelope configurations and photovoltaic integration in different climates, J. Build. Eng. 39 (2021), https://doi.org/10.1016/j.jobe.2021.102292.
[17] P. Zhuk, Lifecycle assessment of vacuum heat-insulation, in: IOP Conf. Ser. Mater. Sci. Eng., Institute of Physics Publishing, 2018, https://doi.org/10.1088/1757-899X/365/3/032012.
[18] S. Verma, H. Singh, Predicting the conductive heat transfer through evacuated perlite based vacuum insulation panels, Int. J. Therm. Sci. 171 (2022), https://doi.org/10.1016/j.ijthermalsci.2021.107245.
[19] Renato Sarc, Roland Pomberger, Magdalena Prommegger, Stefan Eferdinger, Recycling of Cooling and Freezing Appliances Containing Vacuum Insulation Panels (Vips), 2013. http://www.ceced.org/. (Accessed 20 February 2023).
[20] G. Sonnemann, B. Vigon, M. Rack, S. Valdivia, Global guidance principles for life cycle assessment databases: development of training material and other implementation activities on the publication, Int. J. Life Cycle Assess. 18 (2013) 1169–1172, https://doi.org/10.1007/s11367-013-0563-7.
[21] R. Zhang, Z. Shen, B. Park, T. Feng, A. Aldykiewicz, A. Desjarlais, D. Hun, S. Shrestha, Natural fibers as promising core materials of vacuum insulation panels, Constr. Build. Mater. 453 (2024), https://doi.org/10.1016/j.conbuildmat.2024.138890.
[22] X. Dong, Q. Zhang, Y. Lan, Q. Zeng, M. Fan, L. Chen, W. Zhao, Preparation and characterization of vacuum insulation panels with hybrid composite core materials of bamboo and glass fiber, Ind. Crops Prod. 188 (2022) 115691, https://doi.org/10.1016/j.indcrop.2022.115691.
[23] L. Wang, Y. Yang, Z. Chen, Y. Hong, Z. Chen, J. Wu, Preparation and characterization of a type of green vacuum insulation panel prepared with straw core material, Materials 13 (2020) 1–16, https://doi.org/10.3390/ma13204604.
[24] W. Zhao, W. Yan, Z. Zhang, H. Gao, Q. Zeng, G. Du, M. Fan, Development and performance evaluation of wood-pulp/glass fibre hybrid composites as core materials for vacuum insulation panels, J. Clean. Prod. 357 (2022), https://doi.org/10.1016/j.jclepro.2022.131957.
[25] B. Wang, Z. Li, X. Qi, N. Chen, Q. Zeng, D. Dai, M. Fan, J. Rao, Thermal Insulation Properties of Green Vacuum Insulation Panel Using Wood Fiber as Core Material, 2019.

[26] International Organization for Standardization, ISO 14040:2006 – Environmental Management – Life Cycle Assessment – Principles and Framework, 2006. Geneva.
[27] T. Raad, S. Verma, H. Singh, Tree waste based advanced thermal insulation – vacuum insulation panels – for application at up to 70 °C, Int. J. Therm. Sci. 200 (2024), https://doi.org/10.1016/j.ijthermalsci.2024.108971.
[28] HFM 446 Lambda Medium Eco-Line - NETZSCH Analyzing & Testing, 2025. https://analyzing-testing.netzsch.com/en/products/thermal-conductivity/hfm-446-lambda-eco-line-medium. (Accessed 15 March 2025).
[29] N. Pargana, M.D. Pinheiro, J.D. Silvestre, J. de Brito, Comparative environmental life cycle assessment of thermal insulation materials of buildings, Energy Build. 82 (2014) 466–481, https://doi.org/10.1016/j.enbuild.2014.05.057.
[30] P. Jóvári, G. Mészáros, L. Pusztai, E. Sváb, The structure of liquid tetrachlorides CCl4, SiCl4, GeCl4, TiCl4, VCl4, and SnCl4, J. Chem. Phys. 114 (2001) 8082–8090, https://doi.org/10.1063/1.1355998.
[31] A.-M. Tillman, Significance of decision-making for LCA methodology, Environ. Impact Assess. Rev. 20 (2000) 113–123, https://doi.org/10.1016/S0195-9255(99)00035-9.
[32] D.L. Schrijvers, P. Loubet, G. Sonnemann, Developing a systematic framework for consistent allocation in LCA, Int. J. Life Cycle Assess. 21 (2016) 976–993, https://doi.org/10.1007/s11367-016-1063-3.
[33] E.P.A. Danish, Market information in life cycle assessment Bo weidema 2.-0 LCA consultants. https://www2.mst.dk/Udgiv/publications/2003/87-7972-991-6/pdf/87-7972-992-4.pdf, 2003. (Accessed 3 January 2023).
[34] R. Hischier, B. Weidema, H.-J. Althaus, C. Bauer, G. Doka, R. Dones, R. Frischknecht, S. Hellweg, S. Humbert, N. Jungbluth, T. Köllner, Y. Loerincik, M. Margni, T. Nemecek, Swiss Centre for Life Cycle Inventories Implementation of Life Cycle Impact Assessment Methods, 2010.
[35] E.N. Cen, 15804: 2012+ A2: 2019 Sustainability of Construction works—Environmental Product Declarations—Core Rules for the Product Category of Construction Products, European Committee for Standardization (CEN), Brussels, Belgium, 2019.
[36] S. Resalati, T. Okoroafor, P. Henshall, N. Simões, M. Gonçalves, M. Alam, Comparative life cycle assessment of different vacuum insulation panel core materials using a cradle to gate approach, Build. Environ. 188 (2021), https://doi.org/10.1016/j.buildenv.2020.107501.

References

[37] Evonik Industries, Invented to Improve® AEROSIL® for Adhesives and Sealants, 2006.
[38] D.M. Driver, H.L. Seegmiller, Features of a reattaching turbulent shear layer in divergent channelflow, AIAA J. 23 (1985) 163–171, https://doi.org/10.2514/3.8890.
[39] N. Goyer, Performance of painting booths equipped with down-draft ventilation, Am. Ind. Hyg. Assoc. J. 56 (1995) 258–265, https://doi.org/10.1080/15428119591017097.
[40] IPCC, The earth's energy budget, climate feedbacks and climate sensitivity, in: Climate Change 2021 – the Physical Science Basis, Cambridge University Press, 2023, pp. 923–1054, https://doi.org/10.1017/9781009157896.009.
[41] Mercedes-Benz, Truck euro VI transmissions. https://www.mercedes-benz-trucks.com/gb/en/trucks/eactros-600.html, 2023. (Accessed 15 March 2023).
[42] M.A. Barlaz, Forest products decomposition in municipal solid waste landfills, Waste Management (2006) 321–333, https://doi.org/10.1016/j.wasman.2005.11.002.
[43] mikeinlondon, Net Zero Strategy: Build Back Greener, 2021.